AD-A155 845 TURBULENT STRUCTURE OF STABLY STRATIFIED NOCTURNAL SLOPE FLOWS(U) BATTELLE PACIFIC NORTHWEST LAB RICHLAND WA J C DORAN ET AL. APR 85 ARO-19862.2-GS 1/1

UNCLASSIFIED DAAG29-83-K-0052 F/G 20/4 NL

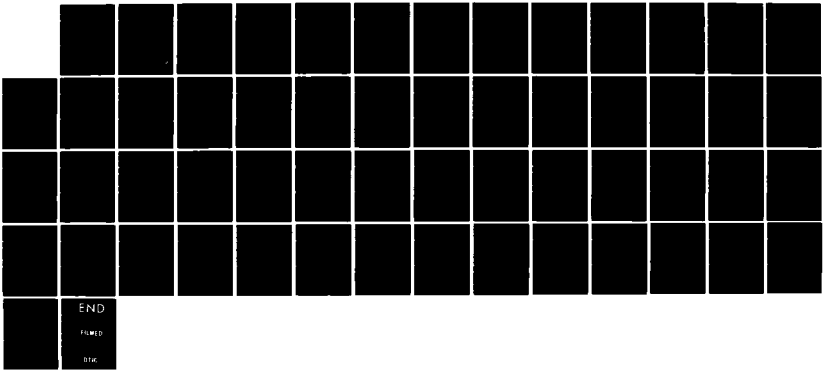

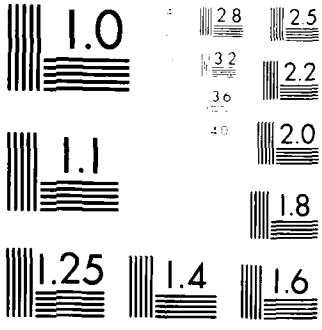
1.0
2.8
2.5
3.2
2.2
3.6
2.0
1.1
1.8
1.25
1.4
1.6

Turbulent Structure of Stably Stratified Nocturnal Slope Flows

Final Report

J. C. Doran
T. W. Horst

April 1985

Prepared for the
U.S. Army Research Office
Research Triangle Park, NC 27709
under Contract 2311105431

Battelle, Pacific Northwest Laboratories
Richland, Washington 99352

Approved for Public Release;
Distribution Unlimited.

LEGAL NOTICE

This report was prepared by Battelle as an account of sponsored research activities. Neither Sponsor nor Battelle nor any person acting on behalf of either:

MAKES ANY WARRANTY OR REPRESENTATION, EXPRESS OR IMPLIED, with respect to the accuracy, completeness, or usefulness of the information contained in this report, or that the use of any information, apparatus, process, or composition disclosed in this report may not infringe privately owned rights; or

Assumes any liabilities with respect to the use of, or for damages resulting from the use of, any information, apparatus, process, or composition disclosed in this report.

The views, opinions, and/or findings contained in this report are those of the authors and should not be construed as an official Department of the Army position, policy, or decision, unless so designated by other documentation.

UNCLASSIFIED

SECURITY CLASSIFICATION OF THIS PAGE (When Data Entered)

REPORT DOCUMENTATION PAGE		READ INSTRUCTIONS BEFORE COMPLETING FORM
1. REPORT NUMBER ARO 19862.2-GS	2. GOVT ACCESSION NO. N/A AD-A155845	3. RECIPIENT'S CATALOG NUMBER N/A
4. TITLE (and Subtitle) Turbulence Structure of Stably Stratified Nocturnal Slope Flows Final Report		5. TYPE OF REPORT & PERIOD COVERED Final report March 1, 1983-February 28, 1985 6. PERFORMING ORG. REPORT NUMBER
7. AUTHOR(s) J.C. Doran T.W. Horst		8. CONTRACT OR GRANT NUMBER(s) DAAG29-83-K-0052
9. PERFORMING ORGANIZATION NAME AND ADDRESS Battelle, Pacific Northwest Laboratories Box 999, Richland, WA 99352		10. PROGRAM ELEMENT, PROJECT, TASK AREA & WORK UNIT NUMBERS
11. CONTROLLING OFFICE NAME AND ADDRESS U. S. Army Research Office Post Office Box 12211 Research Triangle Park, NC 27709		12. REPORT DATE April 1985 13. NUMBER OF PAGES 52
14. MONITORING AGENCY NAME & ADDRESS(if different from Controlling Office)		15. SECURITY CLASS. (of this report) Unclassified 15a. DECLASSIFICATION/DOWNGRADING SCHEDULE

16. DISTRIBUTION STATEMENT (of this Report)

Approved for public release; distribution unlimited.

17. DISTRIBUTION STATEMENT (of the abstract entered in Block 20, if different from Report)

NA

18. SUPPLEMENTARY NOTES

The view, opinions, and/or findings contained in this report are those of the author(s) and should not be construed as an official Department of the Army position, policy, or decision, unless so designated by other documentation.

19. KEY WORDS (Continue on reverse side if necessary and identify by block number)

Slope flows
Drainage winds
Turbulence
Complex terrain

20. ABSTRACT (Continue on reverse side if necessary and identify by block number)

This report describes the results of a 2-year project designed to study turbulence characteristics of wind and temperature fields in drainage flows over a simple slope. Data were collected on a section of Rattlesnake Mountain, a simple, nearly two-dimensional ridge with little vegetation. Propeller anemometers, aspirated thermistors, sonic anemometers and fast response platinum resistance thermometers were used to collect mean and turbulent wind and temperature data 150 m below the ridgeline.

DD FORM 1 JAN 73 1473 EDITION OF 1 NOV 65 IS OBSOLETE

UNCLASSIFIED

SECURITY CLASSIFICATION OF THIS PAGE (When Data Entered)

Evidence for katabatically driven winds was found for a wide range of ambient conditions whenever a surface inversion was formed. When a velocity jet characteristic of good slope flows was present, the vertical profiles of turbulence were found to differ significantly from those found over flat terrain, with the turbulent kinetic energy no longer a monotonically decreasing function of height. Richardson number profiles revealed a value well in excess of critical values ($\sim$0.25) in the region of the jet. The existence of an internal mixing layer, found by other investigators in deeper drainage flows, was not confirmed by our measurements.

Turbulent fluxes were also found to be affected by the formation of a jet in the mean wind. Turbulent momentum fluxes could be either positive or negative, depending on the location of the jet relative to the measurement height. The use of similarity theory, in which surface values of heat and momentum flux are used to scale profiles of wind speed, temperature and turbulent fluxes, does not appear justified. However, scaling of the turbulence by local values of the stress and a locally defined length scale seemed encouraging, although the results were not identical to those found in the literature for flat terrain.

Calculations of turbulent kinetic energy budgets showed a close balance between shear production and viscous dissipation, with buoyancy forces playing a relatively minor role. Above the jet, the contribution from the vertical heat flux was only a few percent of the shear production term and resulted from a near-cancellation of the contributions from the heat flux normal to the sloping surface and the flux parallel to the surface. In this region, the heat flux parallel to the slope was upslope, resulting in an energy production term, while below the jet it was downslope, resulting in an energy loss.

TURBULENCE STRUCTURE OF STABLY STRATIFIED NOCTURNAL SLOPE FLOWS

Final Report

J.C. Doran
T.W. Horst

April 1985

Prepared for the
U.S. Army Research Office
Research Triangle Park, NC 27709
under Contract 2311105431

Battelle, Pacific Northwest Laboratories
Richland, Washington 99352

CONTENTS

FIGURES

FIGURES CONTINUED

TABLES

SUMMARY

This report describes the results of a 2-year project by Battelle, Pacific Northwest Laboratories designed to study turbulence characteristics of wind and temperature fields in drainage flows over a simple slope. Data were collected on a section of Rattlesnake Mountain, a simple, nearly two-dimensional ridge with little vegetation. Propeller anemometers, aspirated thermistors, sonic anemometers, and fast response platinum resistance thermometers were used to collect wind and temperature data on an 18-m tower, 150 m below the ridgeline. Supplementary data were obtained from a second, shorter tower 69 m below the ridgeline and from a tethered balloon used to obtain wind and temperature soundings. The collection of these additional data was funded by the U.S. Department of Energy.

Evidence for katabatically driven winds was found for a wide range of ambient conditions whenever a surface inversion was formed. However, a characteristic jet in the downslope component of the wind was found only when the ambient winds were relatively light. When a jet was present, the vertical profiles of turbulence were found to differ significantly from those found over flat terrain, with the turbulent kinetic energy no longer a monotonically decreasing function of height. Richardson number profiles revealed a value well in excess of critical values ($\sim$0.25) in the region of the jet. The existence of an internal mixing layer, found by other investigators in deeper drainage flows, was not confirmed by our measurements; its absence may possibly be attributed to the shallow nature of the slope flows encountered over Rattlesnake Mountain.

Turbulent fluxes were also found to be affected by the formation of a jet in the mean wind. Turbulent momentum fluxes could be either positive or negative, depending on the location of the jet relative to the measurement height. The use of similarity theory, in which surface values of heat and momentum flux are used to scale profiles of wind speed, temperature, and turbulent fluxes, does not appear justified. However, scaling of the turbulence by local values of the stress and a locally defined length scale seemed encouraging, although the results were not identical to those found in the literature for flat terrain.

Calculations of turbulent kinetic energy budgets showed a close balance between shear production and viscous dissipation, with buoyancy forces playing a relatively minor role. Above the jet, the contribution from the vertical heat flux was only a few percent of the shear production term and resulted from a near cancellation of the contributions from the heat flux normal to the sloping surface and the flux parallel to the surface. In this region, the heat flux parallel to the slope was upslope, resulting in an energy production term, while below the jet it was downslope, resulting in an energy loss.

INTRODUCTION

Terrain can have significant effects on wind and temperature fields, and a description or prediction of such effects can be quite complicated. The work in this project, "Turbulence Structure of Stably Stratified Nocturnal Slope Flows," is a starting point for a systematic approach to the problem of terrain influences; the intent is to study the influence of increasingly complex topography on local wind and temperature structure. In an interim report submitted in April 1984, we described a series of measurements of the mean and turbulent wind and temperature characteristics of nocturnal drainage flows over a simple slope and presented some preliminary descriptions of our results. In this report we discuss our results in detail, extending the analysis given earlier, and summarize our understanding of the principal similarities and differences between stable flows over flat terrain and simple slopes.

The site, instrumentation, and data processing procedures used in this work were described in the interim report and will be reviewed only briefly here. The site for our measurements was a section of Rattlesnake Mountain, near Richland, Washington, that formed a nearly ideal two-dimensional slope. The slope was covered with sparse sagebrush and desert grasses, and extended for nearly 2 km transverse to the downslope direction. The average angle for the first 180 m of vertical drop from the ridge was 21° and decreased rather quickly to 8° below that height. Figure 1 shows a topographical map of the area. The bulk of the measurements discussed in this report were obtained from instruments mounted on an 18-m tower (Tower B) located approximately 150 m below the ridgeline. The mean wind and temperature structure of slope winds was measured by propeller anemometers and aspirated thermistors, respectively. The anemometers were mounted at heights of 0.97, 2.3, 3.6, 5.3, 8.4, 12.9, and 17.9 m, while the thermistors were located at heights of 0.47, 1.2, 2.4, 3.9, 5.4, 8.5, 13.0, and 18.0 m. In addition, two sonic anemometers and two fast-response platinum resistance thermometers were mounted on the tower at heights of 1.9 and 3.2 m to provide turbulence information. Additional details are provided in the interim report.

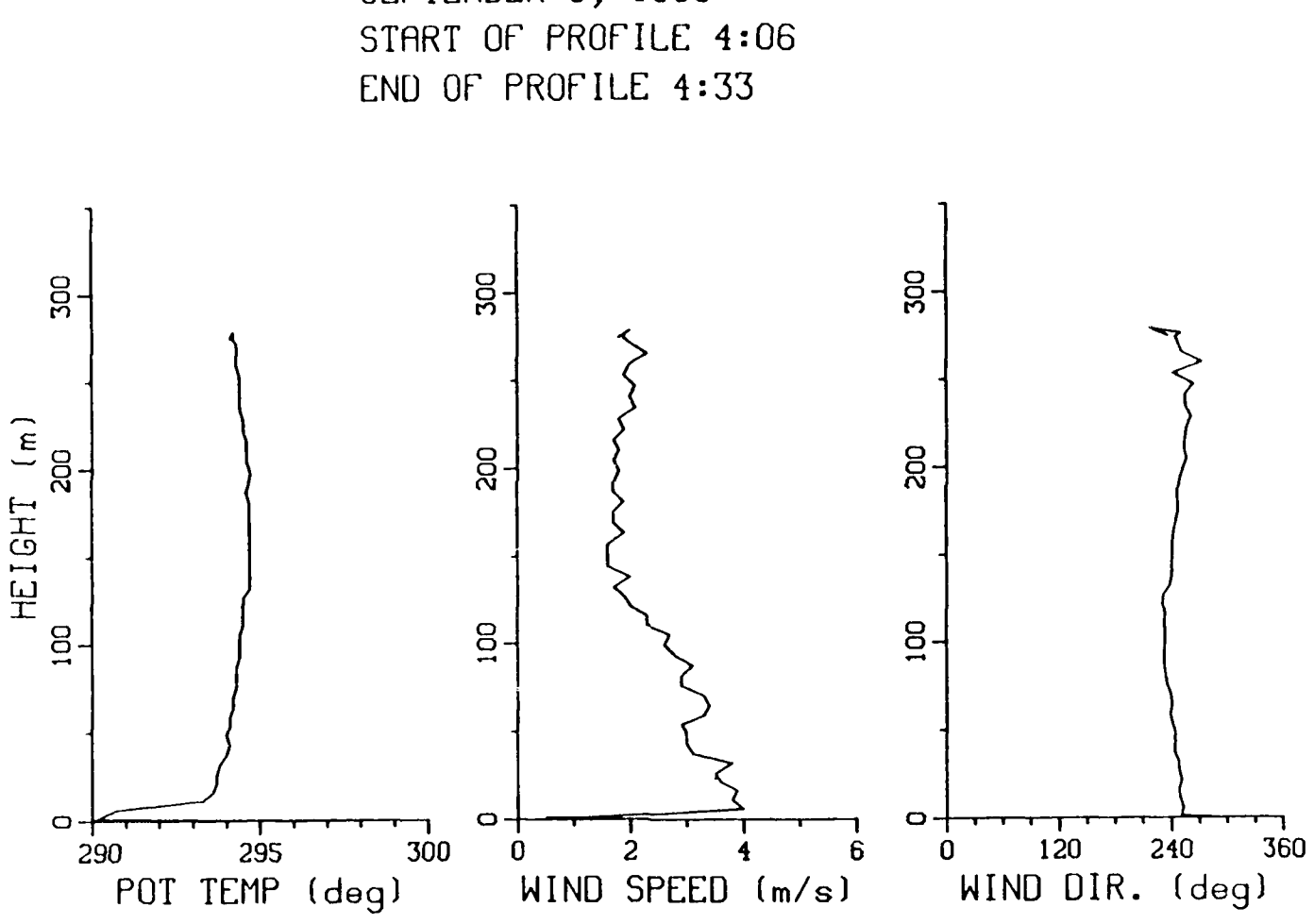

FIGURE 8. Profiles of Wind Speed, Wind Direction, and Potential Temperature Obtained from a Tethered Balloon.

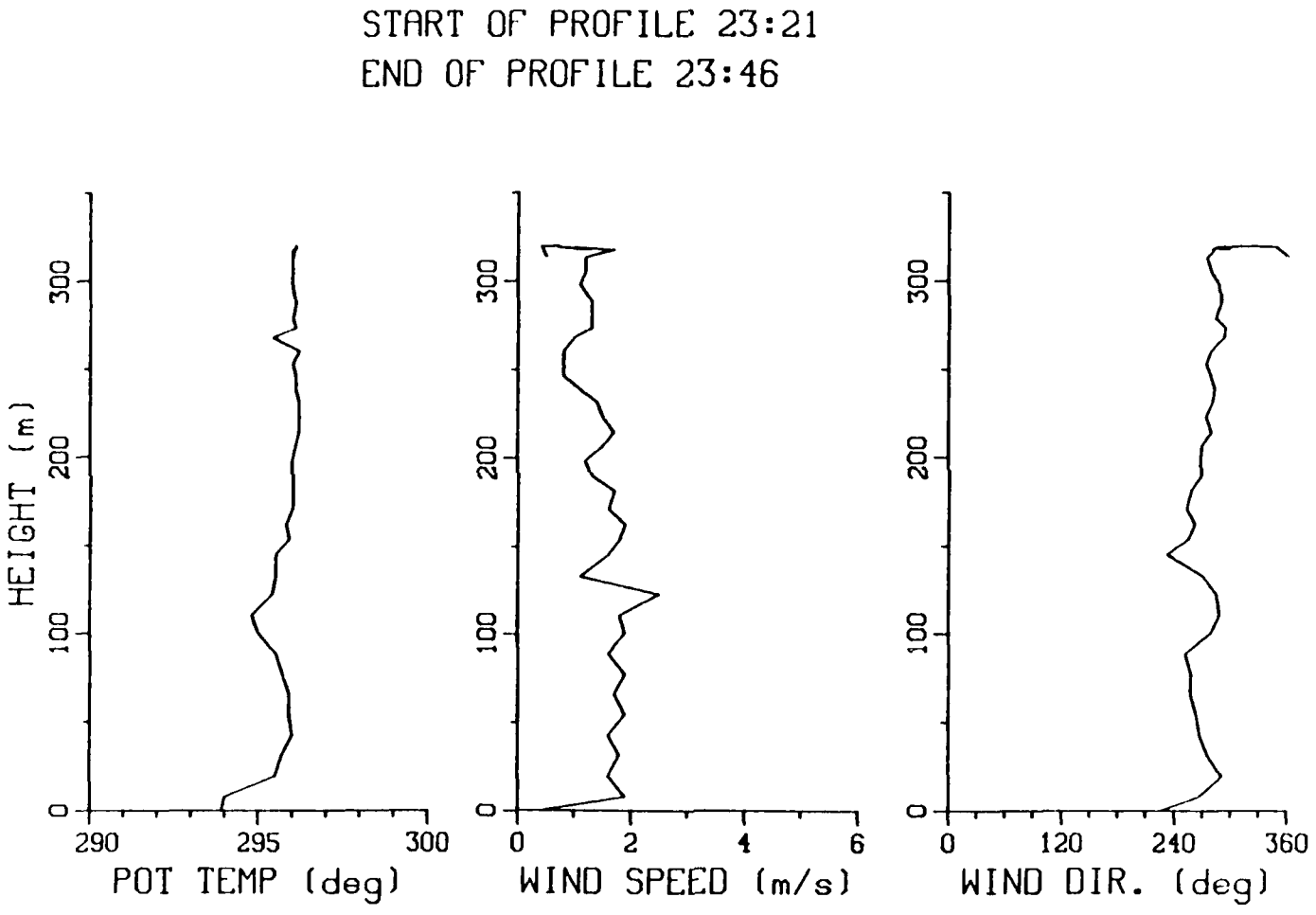

FIGURE 7. Profiles of Wind Speed, Wind Direction, and Potential Temperature Obtained from a Tethered Balloon.

characteristics of the surface-based inversion. Moreover, in a mountain-valley environment, the winds at the level of the ridge top seem a plausible choice for the ambient winds, but over an exposed slope the choice is far more ambiguous.

One possibility is to choose the winds at some upper level as our ambient ones. However, even here the choice is ambiguous as may be seen by considering Figures 7 and 8. These profiles were obtained with a tethered balloon during the early morning hours of September 6, 1983. During the time when the measurements in Figure 7 were obtained, good drainage winds were observed near the surface (e.g., see Figure 6); during the time period covered in Figure 8, the drainage winds had already been eroded. Clearly, the 'ambient' winds below about 150 m, i.e., below ridge height, were significantly higher during the later period than during the earlier one, but the winds above that height were only slightly stronger. Intuitively one might expect that the winds above the ridge top would be a better indicator of ambient conditions that would affect slope flows, but this is not supported by these observations.

In summary, although they can often be obscured by ambient winds, it appears that katabatically driven winds will occur near the surface whenever there is significant surface cooling at night. The depth to which these winds are dominant and the relative amount of shear in wind speed and direction in the first few tens of meters is a complicated function of 'ambient' conditions. The observation of a low-level jet in the downslope wind component seems to preclude the possibility of strong winds aloft, but the absence of strong winds above some arbitrary height does not necessarily imply the development of well-defined drainage winds below. There seems to be no simple criterion by which one can predict the presence or absence of slope winds; instead, numerical multilayer models [2-5] or layer-averaged models [6-7] may be required, and even these cannot be regarded as totally satisfactory.

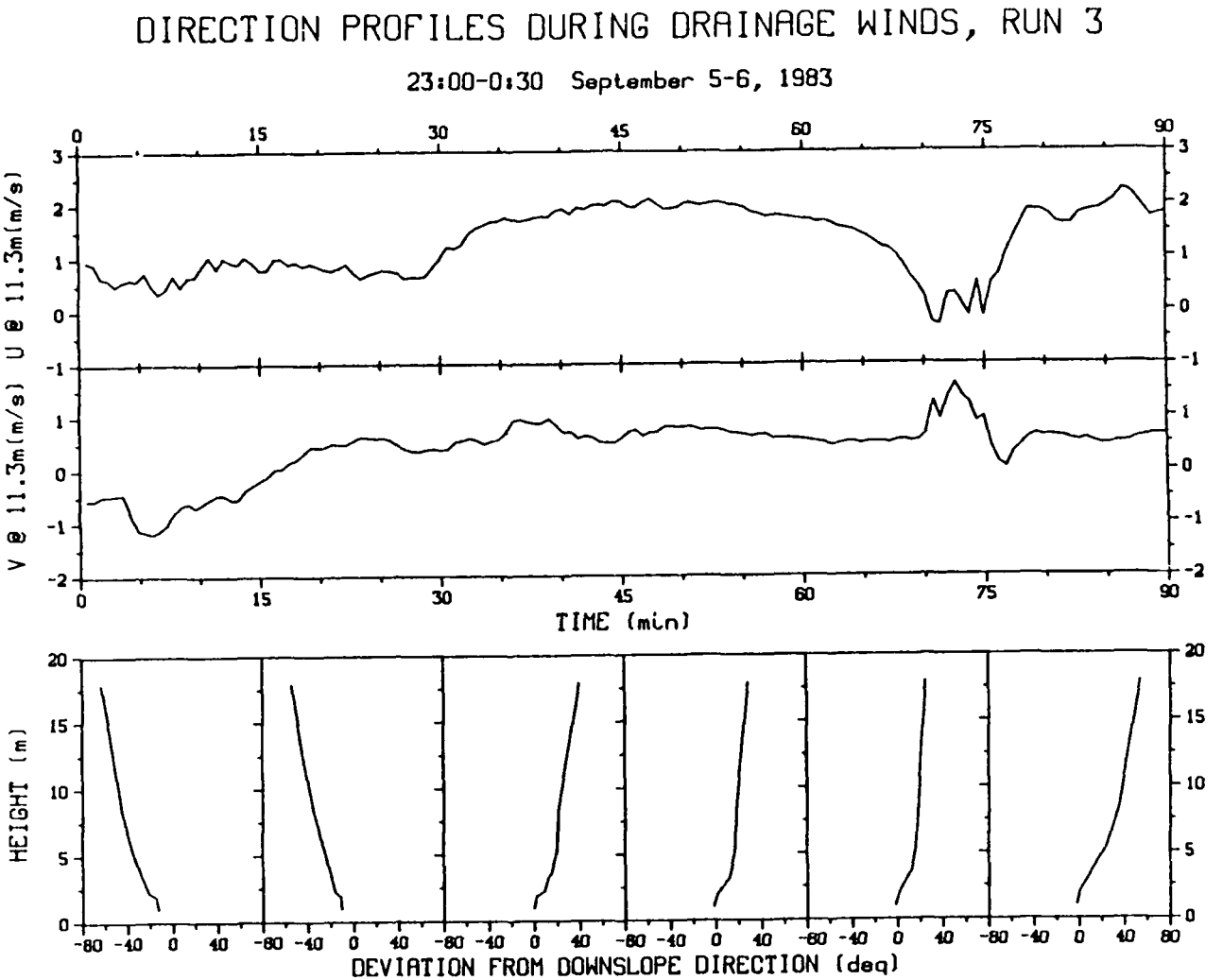

FIGURE 6. Downslope Wind Speed at 11.3 m (Top), Cross-Slope Wind Speed at 11.3 m (Middle), and Profiles of 15 Minute Averages of Wind Directions During Good Drainage Conditions, September 5-6, 1983.

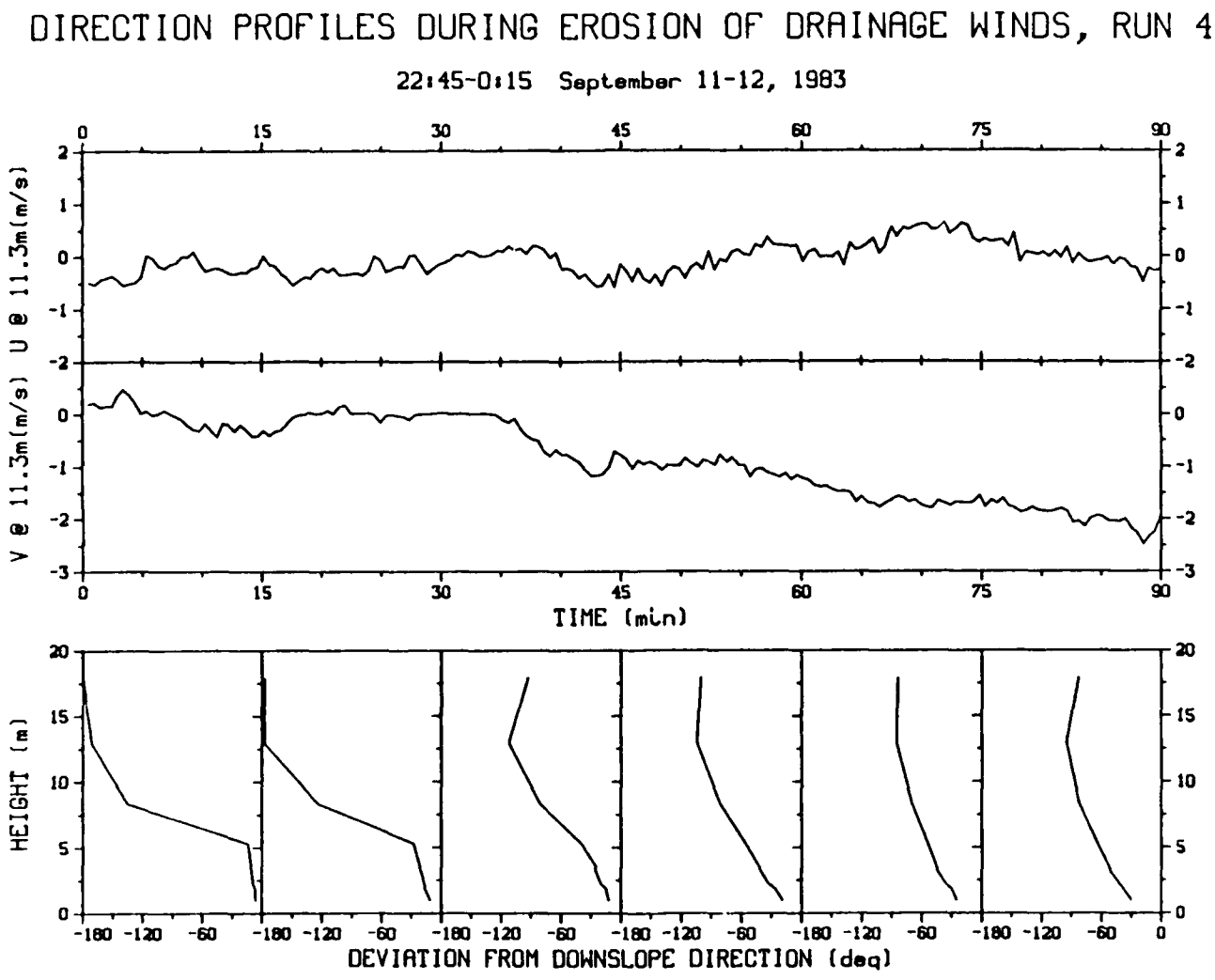

FIGURE 5. Downslope Wind Speed at 11.3 m (Top), Cross-Slope Wind Speed at 11.3 m (Middle), and Profiles of 15 Minute Averages of Wind Directions During the Erosion of Drainage Winds, September 11-12, 1983.

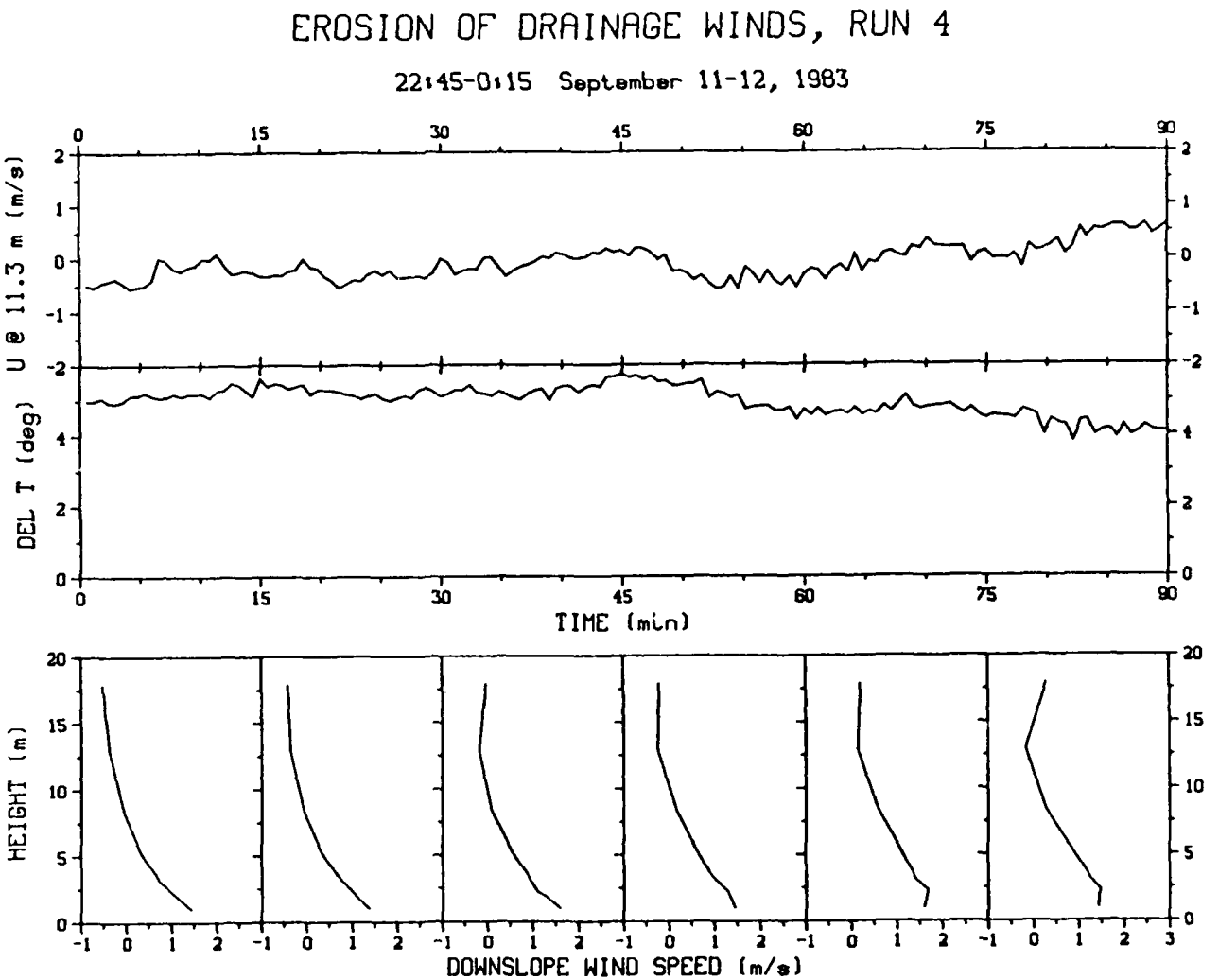

FIGURE 4. Downslope Wind Speed at 11.3 m (Top), T(18 m)-T(Ground) (Middle), and Profiles of 15 Minute Averages of Downslope Wind Speeds (Bottom) During the Erosion of Drainage Winds, September 11-12, 1983.

poor drainage conditions there may still be a significant angle between the local wind direction and the downslope direction, but during good drainage conditions the winds near and below the jet tend to be directed straight down the slope regardless of the direction higher up. Figure 4 shows the jet structure during the beginnings of the erosion of the drainage winds for the night of September 11-12, 1983, and Figure 5 shows how the wind directions at the lowest levels tend to remain downslope during this time. Figure 6 shows examples of wind direction profiles for good drainage conditions.

Figures 2 and 3 also suggest that a somewhat higher ambient wind is necessary to erode drainage winds, once they are established, than was required to prevent their establishment. This requirement may result from the stronger inversion, which reduces the coupling to the upper-level winds, that exists during the erosion phase. However, additional data from other sites are necessary to confirm this hypothesis.

We noted earlier that the inversion depth tends to be about 5% of the vertical drop from the ridge top. In Figures 2 through 6 we have arbitrarily chosen to show the wind speeds at 7.5% of the vertical drop or about 1.5 inversion depths. This is a convenient representation of 'upper-level' winds in the drainage layer, but winds at this level are still almost certainly influenced by katabatic effects and should not be construed as 'ambient'.

It is difficult to define quantitatively a set of ambient conditions that determine whether slope winds will form. Garrett [2] has discussed quantities such as atmospheric water vapor content and cloud cover, and has used a numerical model to estimate how the strength and depth of the slope flows will vary as a result of changes in these factors. A more complicated factor is the role of the ambient wind. Not only do slope winds exhibit a continuous rather than a discrete range of behavior, but it is also unclear how to separate the katabatically induced winds from the 'external' or ambient winds. Horst and Doran[a] correlated the occurrence of slope winds in a protected basin with a dimensionless number S that is a function of the depth and strength of the inversion and the ridge-top wind speed. However, S is, to some degree, diagnostic rather than prognostic because it depends on the

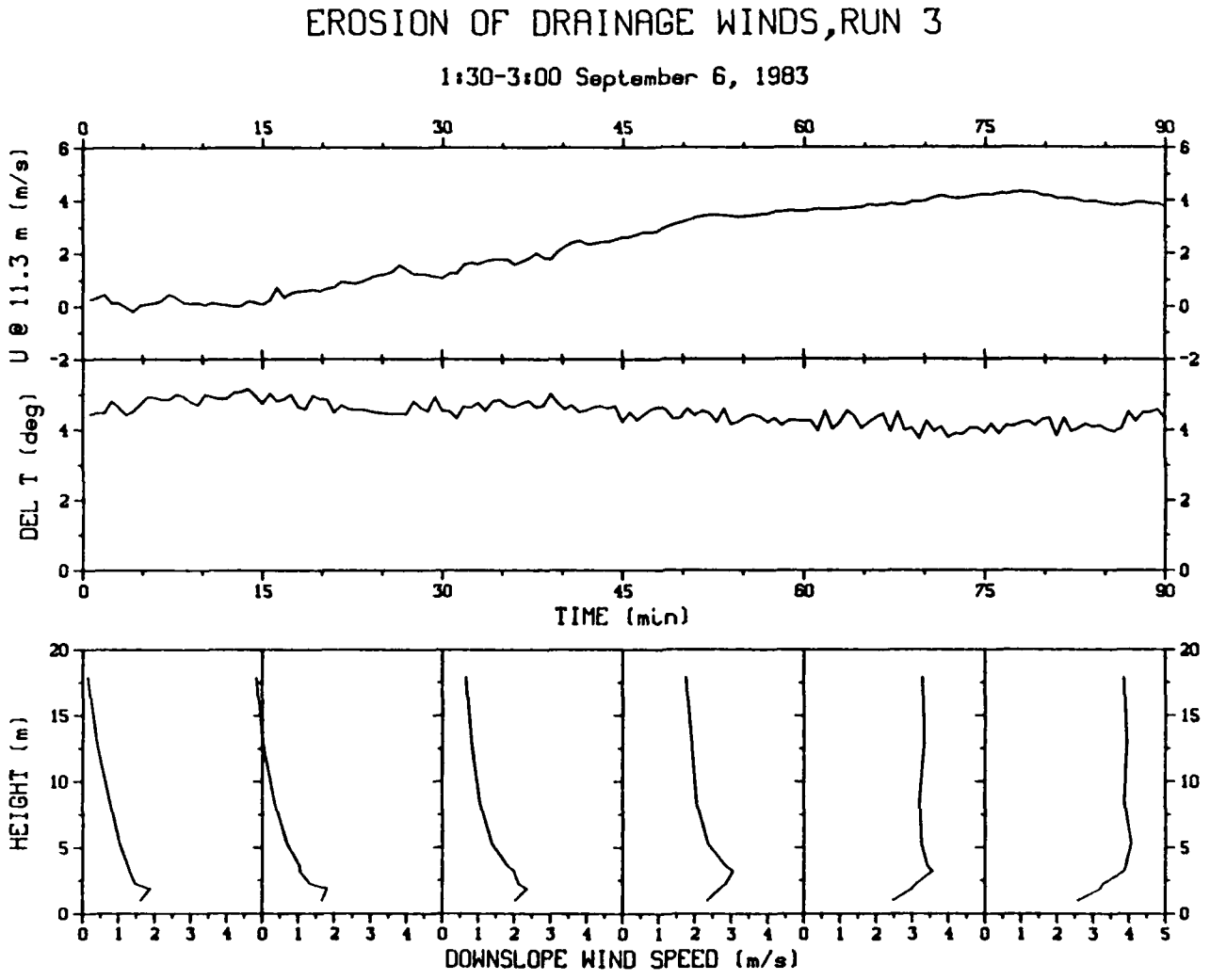

FIGURE 3. Downslope Wind Speed at 11.3 m (Top), T(18 m)-T(Ground) (Middle), and Profiles of 15 Minute Averages of Downslope Wind Speeds (Bottom) During the Erosion of Drainage Winds, September 6, 1983.

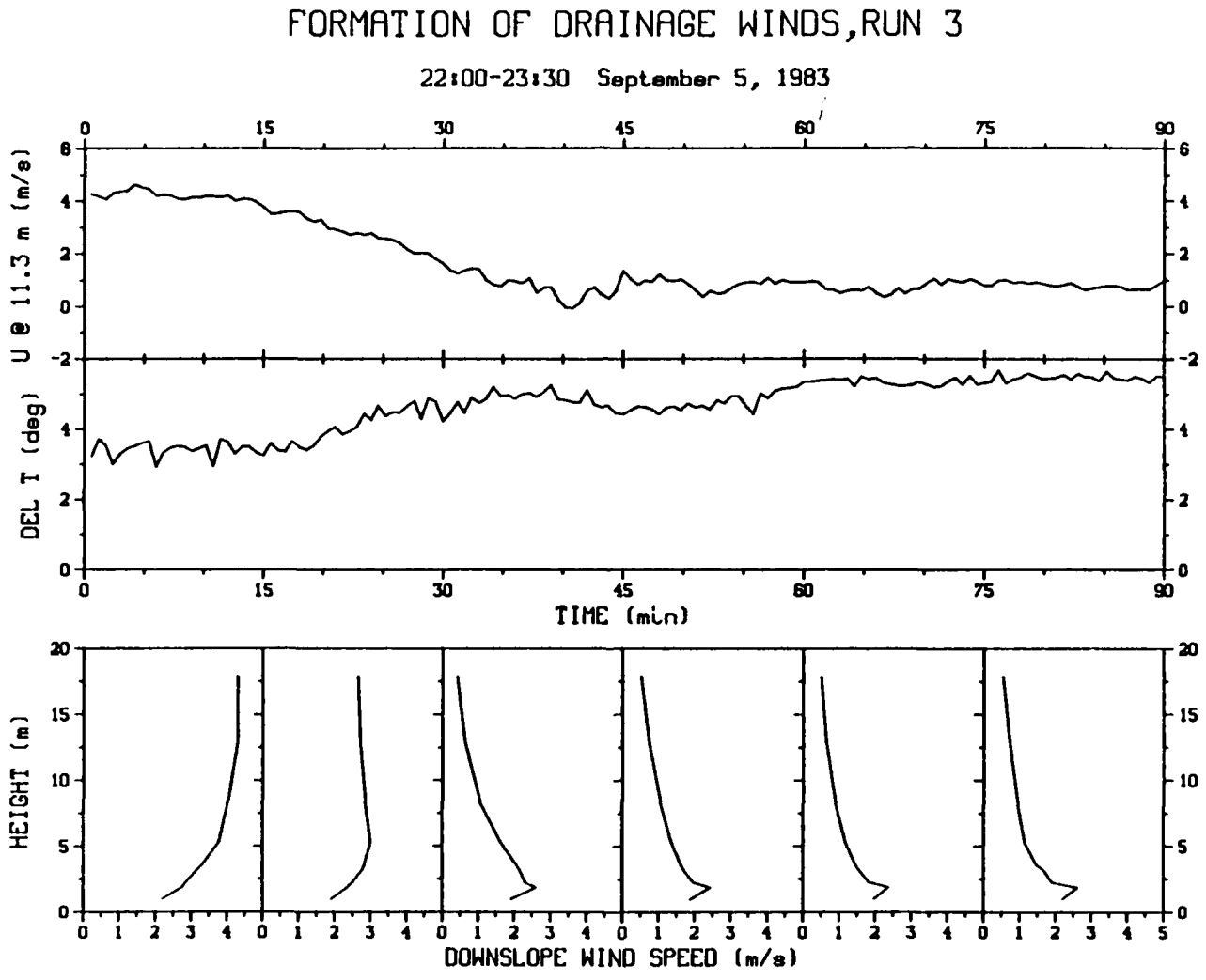

FIGURE 2. Downslope Wind Speed at 11.3 m (Top), T(18 m)-T(Ground) (Middle), and Profiles of 15 Minute Averages of Downslope Wind Speeds (Bottom) During the Formation of Drainage Winds, September 5, 1983.

TEMPORAL DEVELOPMENT

While drainage flows may persist for many hours, they often exhibit significant nonstationary behavior during that time. For example, evidence exists [1] that drainage winds in valleys can undergo periodic oscillations that are superimposed on a relatively steady flow. The 'steady' flow can change as well, particularly if the ambient winds are able to erode the drainage layer (Horst and Doran 1985)[(a)]. These variations in the 'steady' flow are even more apparent over exposed slopes such as those on Rattlesnake Mountain, and essentially preclude the study of such oscillations there. In this section we discuss some aspects of the temporal development of slope winds; we further note that this development is closely connected with the evolution of the turbulence structure of drainage winds, as we will show later in the section on turbulence structure.

Any criterion used for determining the presence or absence of slope winds is arbitrary to some extent. However, as a useful, working definition, we will say that slope winds are clearly dominant when three conditions are met: 1) there is a surface-based inversion that extends to some height h; 2) a maximum in the downslope wind component exists at a height on the order of 0.5 h or less; and 3) the wind direction at and below this maximum lies within 20° of the downslope direction. Under such conditions, slope winds may be regarded as the dominant local circulation system.

With these criteria in mind, consider Figures 2 and 3, which show the formation and erosion, respectively, of slope winds on the night of September 5-6, 1983. The strength of the temperature inversion increases noticeably during the formation of the slope winds, but decreases only slightly during the erosion. Another apparent feature, particularly during the formation phase, is that the winds in the lower portion of the inversion do not change much. Instead, the jet appears when the upper-level winds decrease but tends to be obscured when the upper-level winds increase again. This suggests that the influence of katabatic forces may be more common than might be concluded simply from the presence or absence of a well-defined jet in the wind. A good indicator of this influence is the directional shear of the winds. As the surface is approached, the winds shift toward a downslope direction. Under

kinetic energy need not be a monotonic function of height. In particular, in the region of the maximum in the downslope wind component, the turbulence production may become quite small. The stable stratification inhibits vertical exchange of heat and momentum, and above the wind maximum the flows can be largely decoupled from surface influences. While decoupling occurs over flat terrain as well, it can occur at much lower heights in drainage winds because the local maximum in the wind speed often occurs close to the surface. We shall examine examples and implications of these effects throughout this report.

We will generally use the terms 'slope' winds and 'drainage' winds interchangeably. To be more precise, we could distinguish between slope winds flowing down a simple, sloping surface and drainage winds that result from the merging or channeling of slope winds by topographic features. However, in the discussion of the Rattlesnake Mountain results, such a distinction is largely an academic one and will be ignored.

MEAN FLOW CHARACTERISTICS

Because the characteristics of the mean wind and temperature fields are important for an understanding of the turbulence properties, we begin with a brief review of their principal features in drainage flows over simple slopes. Drainage winds form when radiational cooling of the surface cools the air near the slope more than the free air at the same elevation. Observations at several sites show that a surface-based inversion forms with a depth of about 5% of the vertical drop from the top of the slope, and a local maximum in the downslope wind component occurs at a height between 0.2 and 0.5 of the inversion depth (Horst and Doran 1985)[(a)]. The details of the wind profile depend sensitively upon the ambient winds, which can produce significant shears in both wind speed and direction. These shears extend over heights on the order of 10 m at the site of Tower B on Rattlesnake Mountain.

In contrast to this, nocturnal flows over flat terrain tend to form wind and temperature profiles that are described by a log-linear relationship in the boundary layer. Within this layer there is a monotonic increase of wind speed with height and often a considerable height range (~100 m) in which the wind speed and temperature profiles vary nearly linearly with height. While nocturnal jets do form, the wind maxima generally occur well above 100 m, and their formation is not a result of katabatic forcing.

The presence of large shears in slope flows has important implications for their turbulence characteristics. Because the value of the shear production term in the turbulence kinetic energy budget can change rapidly over a small vertical extent, the turbulence in drainage flows can differ significantly from that found in nocturnal flows over flat terrain. For example, the turbulent kinetic energy over flat terrain is nearly constant with height near the surface, decreases with height within the boundary layer, and approaches zero near the top of the layer. In slope flows, the interaction of katabatic and ambient winds can produce complex wind shear profiles and the turbulent

---

(a) Research results conducted by T. W. Horst and J. C. Doran, 1985, "Nocturnal Drainage Flow on Simple Slopes." Accepted for publication in Boundary-Layer Meteorology.

In the next section we describe the mean flow characteristics of slope winds and their implications for the turbulent structure of these flows. We then discuss the temporal development of slope flows and the difficulties encountered in identifying critical ambient conditions that determine the presence or absence of katabatic winds. The atmospheric stability, described in terms of a gradient Richardson number, is examined next, and comparisons with behavior over flat terrain are made. A discussion of turbulence structure follows, with a description of local scaling approaches. The main body of the report concludes with a description of the turbulent kinetic energy budget in a slope flow, and an appendix covers some details of the calculations required in the budget evaluation.

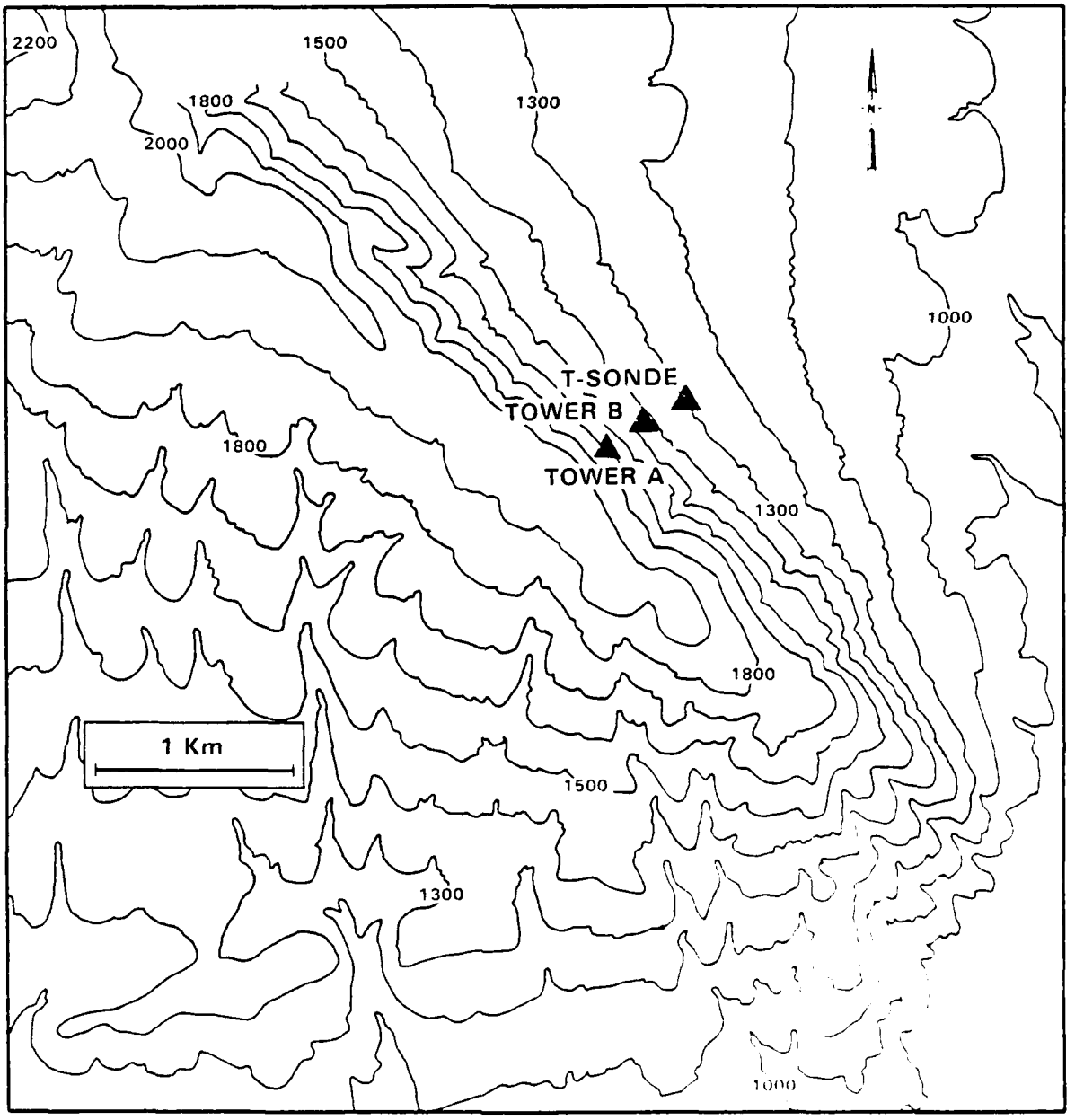

FIGURE 1. Topographical Map of Rattlesnake Mountain Site, Showing Locations of Main Instrument Towers (B), Second Tower (A), and Tethered Sonde. Height Contours are in Feet.

ATMOSPHERIC STABILITY IN SLOPE FLOWS

The local stability of the slope flow layer has important implications for its turbulence structure. A measure of the stability is provided by the gradient Richardson number (Ri), which may be regarded as the ratio of the buoyant production or suppression of turbulence to the shear production. We have calculated vertical profiles of Ri as follows:

$$Ri = \frac{g}{T}\frac{\partial\theta}{\partial z} \Big/ \left\{\left(\frac{\partial U}{\partial z}\right)^2 + \left(\frac{\partial V}{\partial z}\right)^2\right\} \qquad (1)$$

during periods of drainage winds as well as during periods when such winds were not evident. In Equation (1), g is the acceleration of gravity, T is the ambient temperature, $\partial\theta/\partial z$ is the gradient of the potential temperature, and U and V are the mean downslope and cross-slope velocity components, respectively.

If Ri exceeds a critical value, often estimated to be about 0.25, turbulence is strongly suppressed and is generally intermittent or absent. Manins and Sawford [8] found, in their studies of katabatic flows, an internal mixing region, above the height of the wind maximum, in which the wind and temperature profiles were approximately linear and in which Ri was approximately constant with height and equal to a near-critical value of about 0.27. Nieuwstadt [9] presents data that show that in stable layers over flat terrain Ri should approach a constant value ($\sim$0.22) over a considerable height range. Within that range, he showed that the scaling of turbulence is more appropriately done with locally determined values of stress and heat flux, rather than with surface values.

The evaluation of Ri for shallow drainage flows was difficult and frustrating. While temperature profiles were reasonably smooth, the velocity profiles were not, particularly in the region of the jet. In addition, the winds were generally light, so that the differences in speed between two adjacent anemometers were often quite small and the consequent uncertainties in the derivatives of speed with height were rather large. The upshot of this was a large degree of scatter in Ri from one time period to the next, even during nominally steady conditions.

Despite this scatter, we were able to find some consistent structure in the Richardson number profiles. As expected, during good drainage winds the average Richardson number near the jet in the downslope component was larger than the critical value. This feature is consistent with the relatively small turbulent energy found in this region, as discussed in the following section. Immediately above the jet, the Richardson numbers were lower, with values generally less than the critical value. Some suggestion of a smaller, secondary peak in Ri existed around 3.5 m for the nights of September 5-6 and September 11-12, the two nights with the best combination of drainage winds and data recovery. During good drainage periods on these nights, the height of the jet ranged between about 1 and 2 m, while the inversion depths were on the order of 10 m. Above 3.5 m, Ri then fell, only to again increase near or above the 'top' of the inversion. Note that these latter values of Ri are particularly uncertain, because velocity differences of only a few tens of centimeters per second or less, and temperatures differences of 0.1 °C or less, often characterized the wind and temperature profiles above 6 or 7 m. Table 1 summarizes the behavior of Ri for these two nights.

The Richardson number profiles at Rattlesnake Mountain differ significantly from the profiles found over flat terrain, where Ri increases monotonically with height until it reaches a near-critical value. The general decrease of Ri with height was also observed at another slope site, although the height resolution of the measurements was inadequate to detect 'structure' similar to that found on Rattlesnake Mountain. During the late summer and early fall of 1984, we made limited measurements of drainage winds on the sidewall of a large valley at Brush Creek, Colorado. This was part of our effort for the Department of Energy's Project ASCOT (Atmospheric Studies in Complex Terrain). Wind speed, direction, and temperature measurements were made at five levels on a 9.1-m tower located about 450 m below the ridge top on a 34° slope. During good drainage conditions, our maximum wind speeds were observed at the lowest anemometer (2.2 m), indicating a flow in this region that was much shallower than would have been expected from an extrapolation of the results based on the Rattlesnake Mountain data. The calculated Richardson numbers decreased monotonically with height, with values generally exceeding the critical value at our lowest two levels of calculation (3.1 and 4.9 m). Table 2 gives a summary of these results.

TABLE 1. Richardson Numbers in Slope Flows on Rattlesnake Mountain, September 5-6 and September 11-12, 1983. (Standard deviations are shown in parentheses.)

Height (m)	Richardson Number Sept. 5-6	Sept. 11-12
1.5	0.15 (0.08)	0.31 (0.16)
1.75	1.48 (1.14)	0.43 (0.22)
2.0	0.09 (0.08)	0.14 (0.09)
2.5	0.17 (0.09)	0.06 (0.03)
3.5	0.28 (0.19)	0.25 (0.18)
4.0	0.09 (0.09)	0.07 (0.03)
6.5	0.44 (0.45)	0.07 (0.02)
10.0	0.22 (0.21)	0.12 (0.07)
15.0	0.27 (0.13)	0.42 (0.79)

TABLE 2. Richardson Numbers in Slope Flows in Brush Creek, Colorado, September-October, 1984. (Standard deviations are shown in parentheses.)

Height (m)	Richardson Number Sept. 19-20	Sept. 25-26	Sept. 29-30	Sept. 30	Oct. 5-6
3.1	1.60 (0.77)	0.80 (0.54)	1.27 (0.73)	1.25 (0.52)	0.60 (0.20)
4.9	0.32 (0.20)	0.30 (0.34)	0.37 (0.33)	0.60 (0.62)	0.23 (0.22)
6.8	0.21 (0.18)	0.13 (0.17)	0.11 (0.10)	0.25 (0.32)	0.09 (0.10)
7.9	0.12 (0.10)	0.12 (0.12)	0.06 (0.06)	0.10 (0.09)	0.08 (0.08)

McNider and Pielke [10] have suggested that differential temperature advection can actually produce a layer of unstable air above the drainage layer on valley sidewalls. Our Colorado measurements did not show such a layer, but the decrease in Ri with height would be consistent with such an effect if it occurred at elevations greater than our tower height.

Neither the Rattlesnake Mountain data nor the Colorado data support the findings of Manins and Sawford [8] concerning an internal mixing layer in which Ri is constant at a near-critical value. On the other hand, our drainage depths were considerably shallower than theirs, and it is quite possible that the extent of such a mixing layer is too small to be resolved at our sites.

TURBULENCE STRUCTURE

In our discussion of mean flow characteristics, we noted how the presence of a local maximum in the downslope component of the wind speed could affect the production of turbulent kinetic energy and produce vertical profiles of turbulent energy that differ markedly from those found over flat terrain. A review of some of the evidence for such effects follows. Figure 9 shows profiles of mean wind components for three different time periods during the night of September 11-12, 1983. The time span includes most of the period shown in Figure 2 and continues until about 45 min before the periods shown in Figure 3. During the time covered in Figure 9, the cross-slope wind component strengthened from a negligible value to a value large enough to mask the drainage flows, and the wind shear went from a state in which drainage flows were the controlling influence to one in which the ambient winds dominated. At all times, however, a jet could still be observed in the downslope component.

Figures 10 and 11 show spectra of the downslope wind components at three levels for the first and last of the three periods, respectively. During the first period, when there was a well-defined slope flow, the turbulent kinetic energy was higher at the upper levels than at the lowest level, in contrast to the usual behavior found over flat terrain. In the region of the maximum in the downslope wind component ($\sim$1 m), the shear production of turbulence is small because $\partial U/\partial z$ and $\partial V/\partial z$ are both close to zero. Above that region the shear increases, and the turbulent energy is larger. Later in the night the temperature inversion weakened, the downslope component of the wind almost vanished, and the winds were predominantly cross-slope. At that point, the spectra look quite similar to those found over flat terrain, with little difference in turbulent energy among the three levels shown (Figure 11). During periods of strong downslope winds that showed no evidence of being driven by katabatic forces, the spectra also looked similar to those found over level ground. An example is shown in Figure 12.

The direction of the vertical momentum flux can also change, depending on the relative locations of the wind maximum and the observation point. This behavior is shown in Figure 13, which shows uw cospectra for the three time

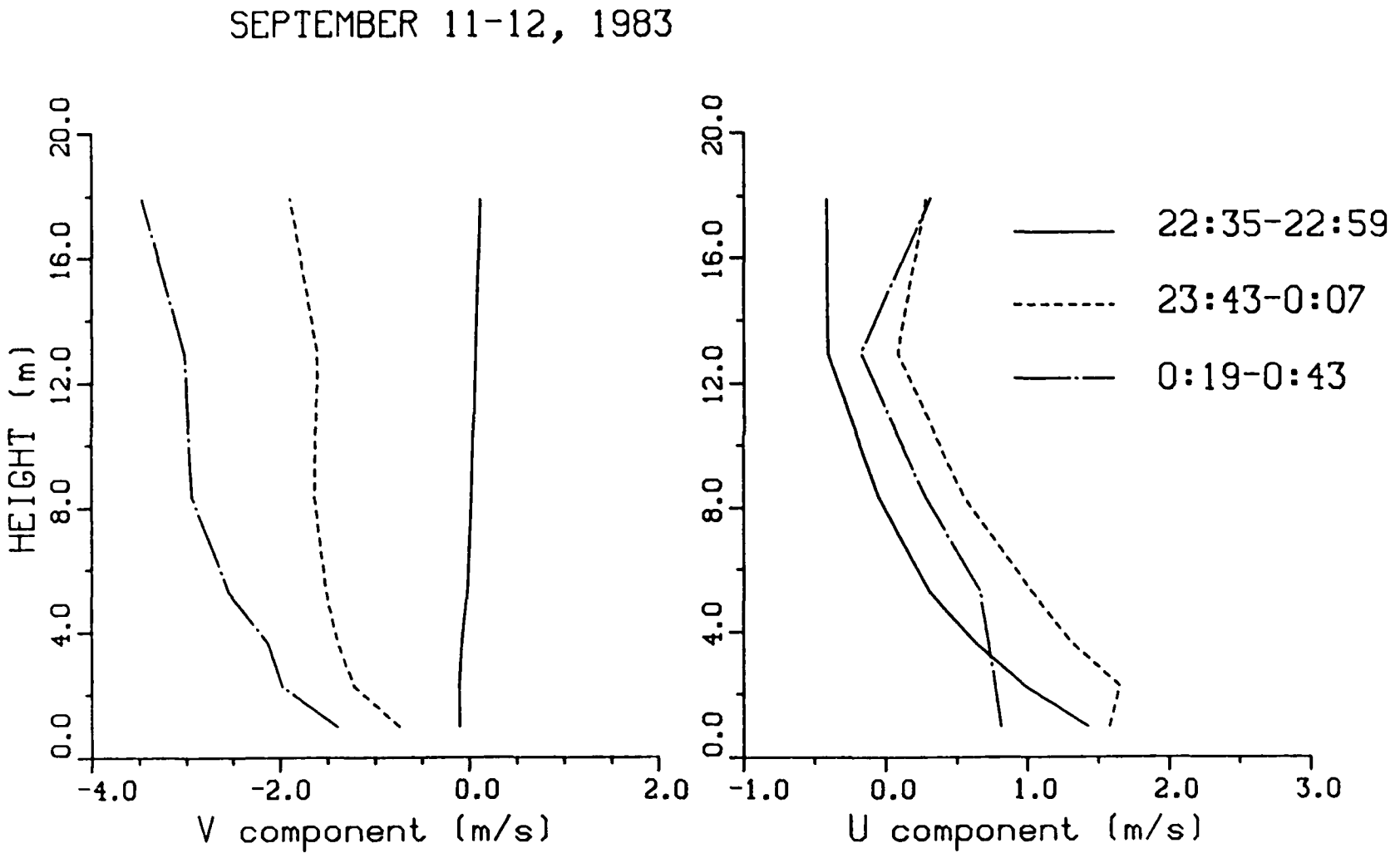

FIGURE 9. Profiles of Cross-Slope Wind (V) and Downslope Wind (U) for Three Time Periods, September 11-12, 1983.

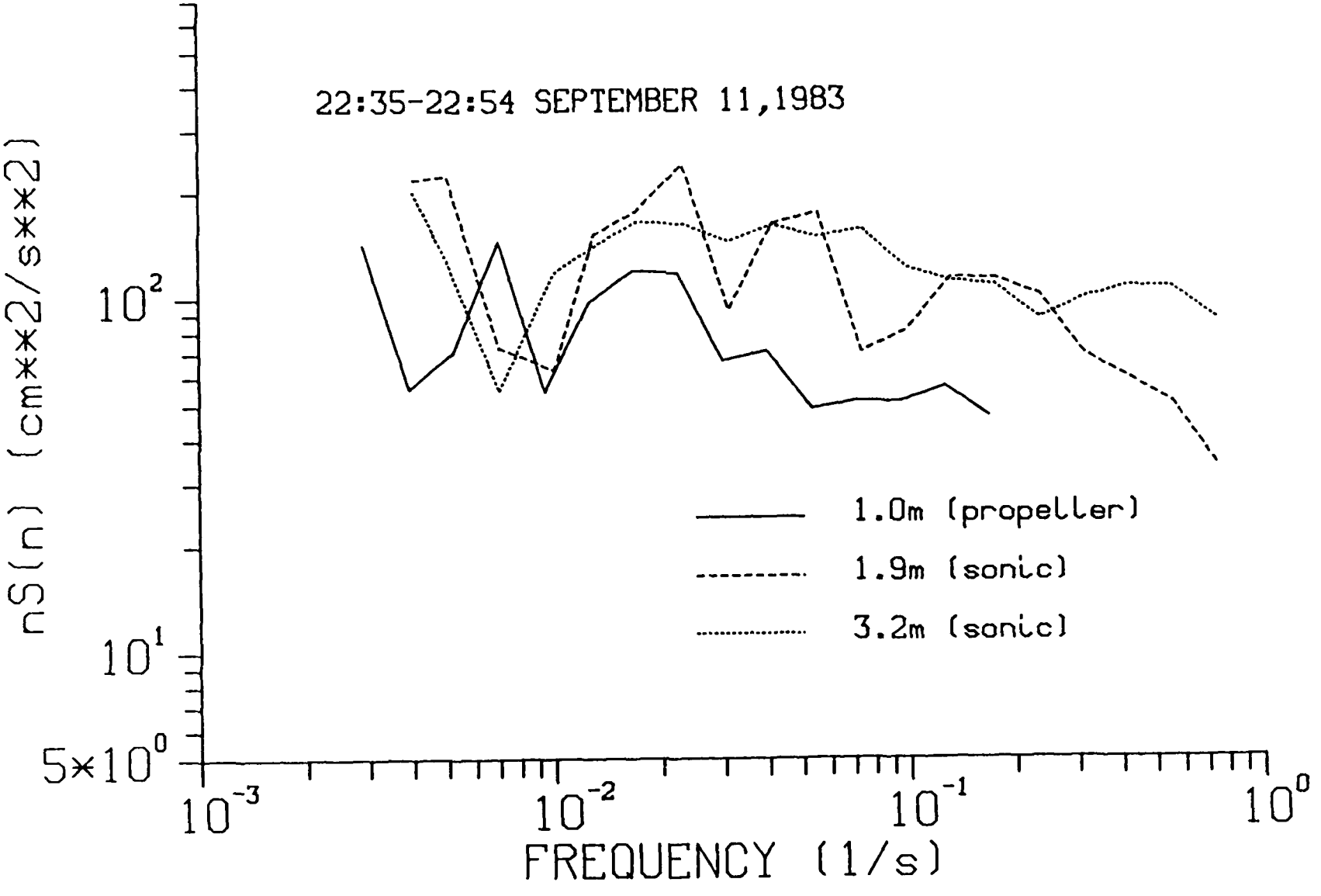

FIGURE 10. Spectra of Mean Wind Parallel to Slope at Three Heights During Good Drainage Conditions, September 11, 1983.

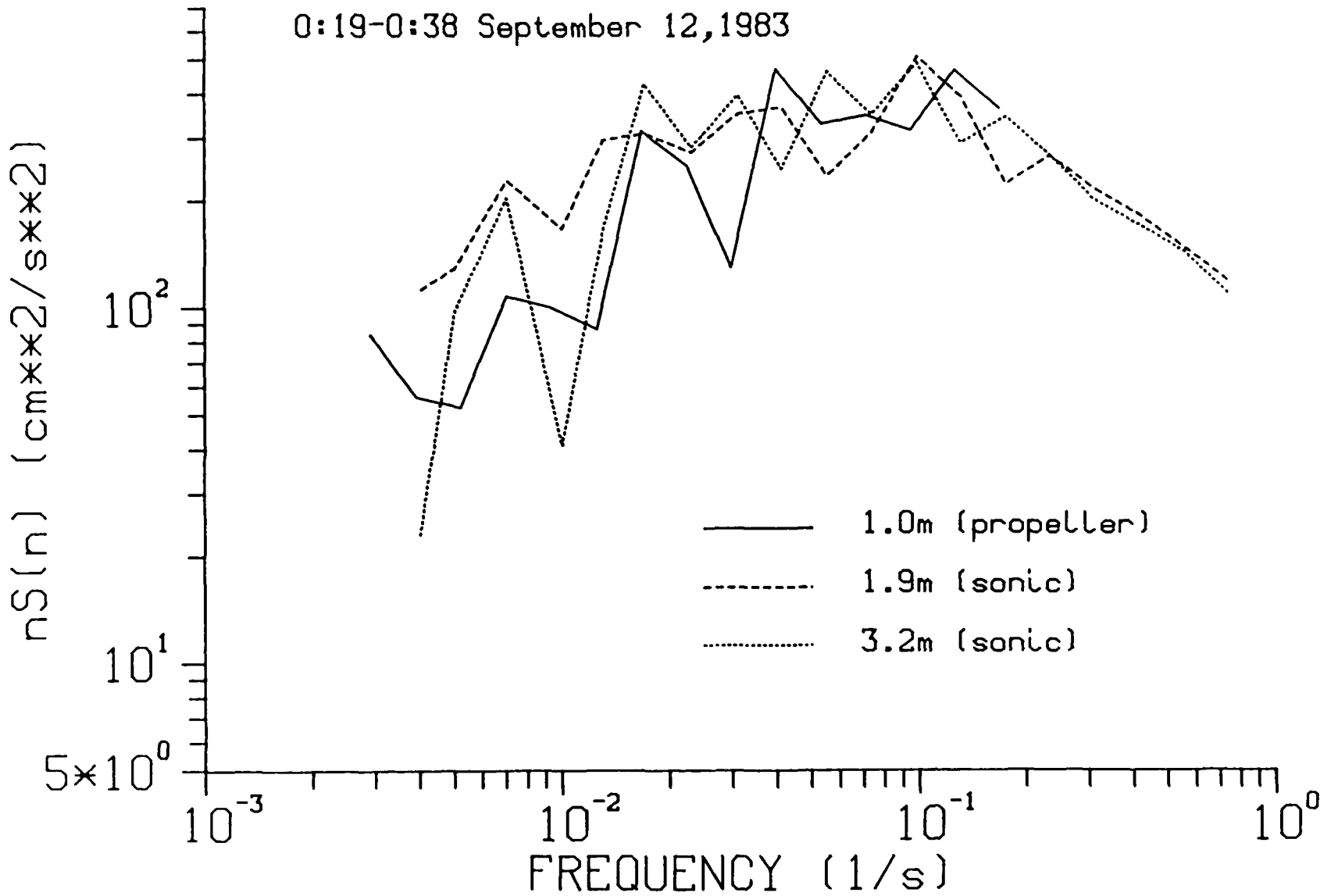

FIGURE 11. Spectra of Mean Wind Parallel to Slope at Three Heights During Poor Drainage Conditions, September 12, 1983.

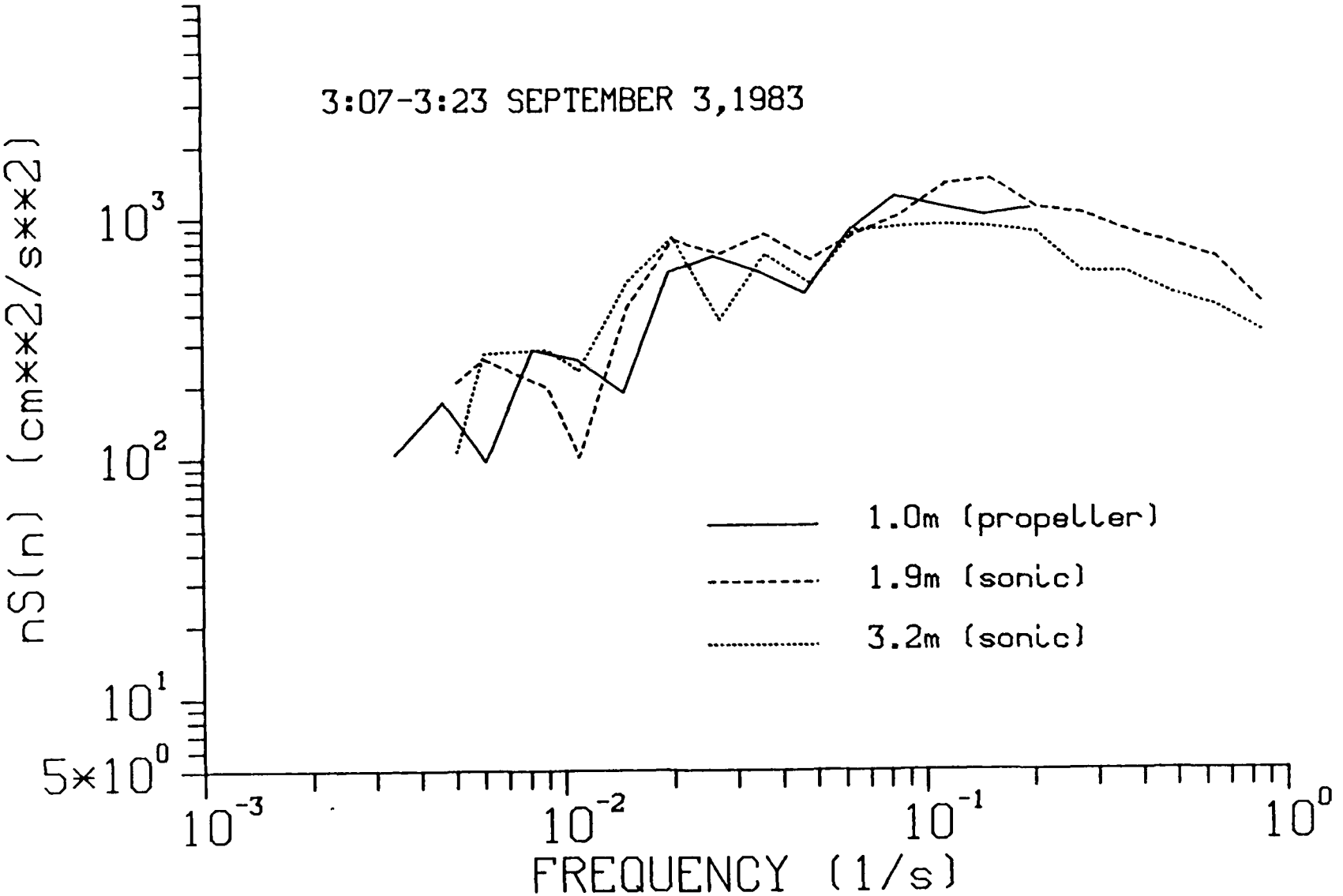

FIGURE 12. Spectra of Mean Wind Parallel to Slope at Three Heights During Strong Wind Period (No Drainage), September 3, 1983.

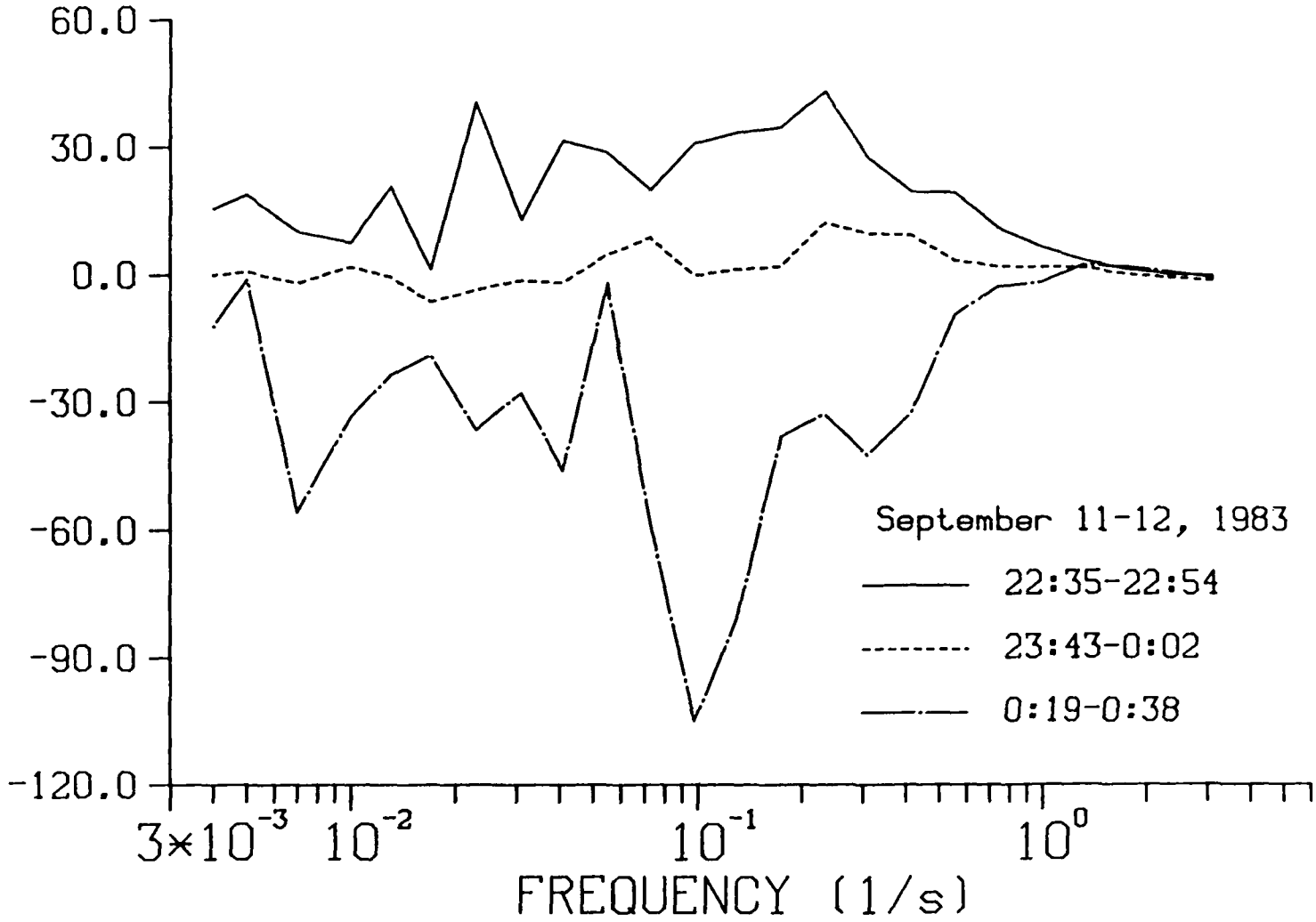

FIGURE 13. Cospectra of u and w at 1.9 m for Three Periods, September 11-12, 1983.

periods mentioned above. (Here, uw is the momentum flux normal to the slope, u is the fluctuating component of the mean wind component parallel to the slope and in the downslope direction, while w is the fluctuating, normal velocity component.) The direction of the momentum flux changed from positive to negative, as indicated by the cospectra, and was consistent with the local vertical gradient of the wind speed. The change in the direction of the momentum flux has implications for the turbulent kinetic energy budget that will be discussed in the next section.

When the momentum flux is upwards, normal surface similarity theory is not expected to be applicable, and the flows above the jet should be largely decoupled from the surface. Nieuwstadt [9] also considered turbulence behavior in stable flows over flat terrain under circumstances in which the flows tended to decouple from the surface, although in his cases $\overline{uw}$ remained negative. In the asymptotic limit of complete decoupling, we obtain 'z-less stratification'; i.e., the turbulence scaling depends only on local parameters and is independent of height above the surface. Although our terrain and the governing equations for the wind and temperature fields differ from those of Nieuwstadt, the common aspect of decoupling suggests that his scaling approach might be a useful one for drainage flows as well, at least in the region above the jet. Accordingly, we chose twenty-eight 15-min periods, from three different nights, during which the momentum flux was positive and analyzed their characteristics in terms of local scaling parameters. The relevant parameters are the local shear stress τ and the length scale Λ, where

$$\tau = \left\{ (\overline{uw})^2 + (\overline{vw})^2 \right\}^{1/2} \qquad (2)$$

and

$$\Lambda = -\tau^{3/2} \, k \, \frac{g}{T} \, \overline{w\theta} \qquad (3)$$

In Equations (2) and (3), u and v are the turbulent downslope and cross-slope velocity components, respectively, k is von Karman's constant, and $\overline{w\theta}$ is the sensible heat flux.

In Figure 14 we show the variation of $\sigma_w/\tau^{1/2}$ with z/Λ, where σ_w is the standard deviation of the vertical velocity fluctuations. In this context, 'vertical' actually refers to a direction normal to the local slope, because the streamlines of the wind are approximately parallel to the terrain close to the surface. The solid points are the experimental values obtained by Nieuwstadt [9] on a 200-m mast at Cabauw, The Netherlands; the line represents the results of his second-order closure model of stable flow over flat terrain; and the open points are experimental values obtained on Rattlesnake Mountain. The data for both Cabauw and Rattlesnake Mountain have been collected into z/Λ classes, and the standard deviations of the measurements about the mean value for each class are also shown. The Cabauw results tend to lie above the model predictions for z/Λ greater than about 0.5, while the Rattlesnake values lie below the predictions for small values of z/Λ and approach the model predictions as z/Λ approaches 1.

Figure 15 shows the variation of $q/\tau^{1/2}$ with z/Λ, where $q^2/2$ is equal to the turbulent kinetic energy. Except for the Rattlesnake Mountain data corresponding to the lowest z/Λ class, the Rattlesnake data and the Cabauw data agree very well; both lie above the model predictions for flat terrain. The data show that the turbulent kinetic energy is proportional to the local shear stress. This is consistent with the turbulence spectra given earlier, which showed reduced levels of turbulent kinetic energy in the vicinity of the velocity jet where shear production is small. We will also show later, in an analysis of turbulence energy budgets, that the buoyancy terms in the slope flows are not a major factor in energy dissipation or production. Instead, shear production and viscous dissipation are approximately in balance, which is consistent with the results shown in Figure 15.

Turbulent exchange processes may be represented in terms of exchange coefficients K_h for heat and K_m for momentum. We define these by

$$K_h = - \overline{w\theta} \Big/ \frac{\partial \theta}{\partial z} \qquad (4)$$

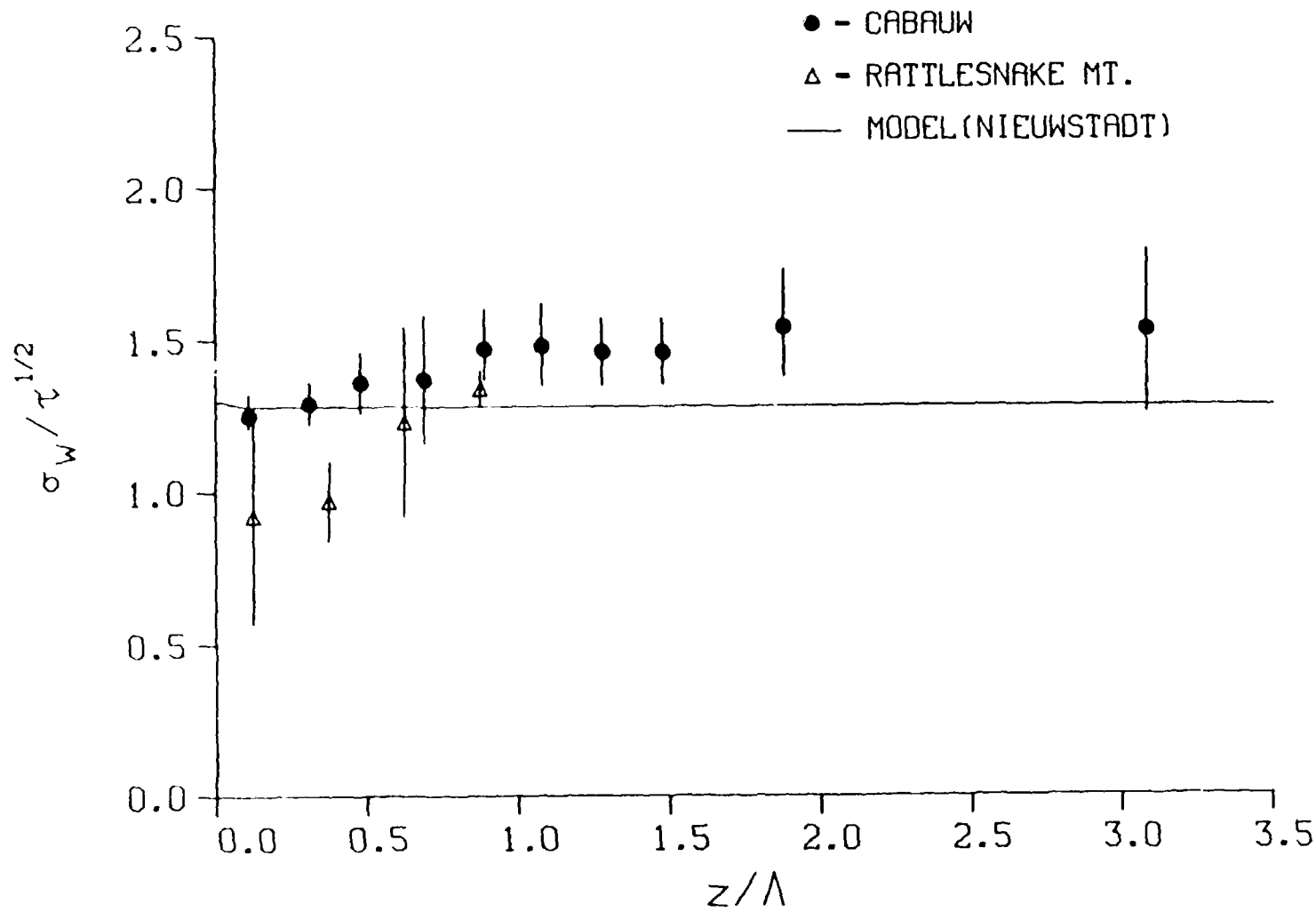

FIGURE 14. $\sigma_w/\tau^{1/2}$ as a Function of z/Λ. Symbols Indicate Averages for Classes of z/Λ, and Vertical Bars Indicate Standard Deviations.

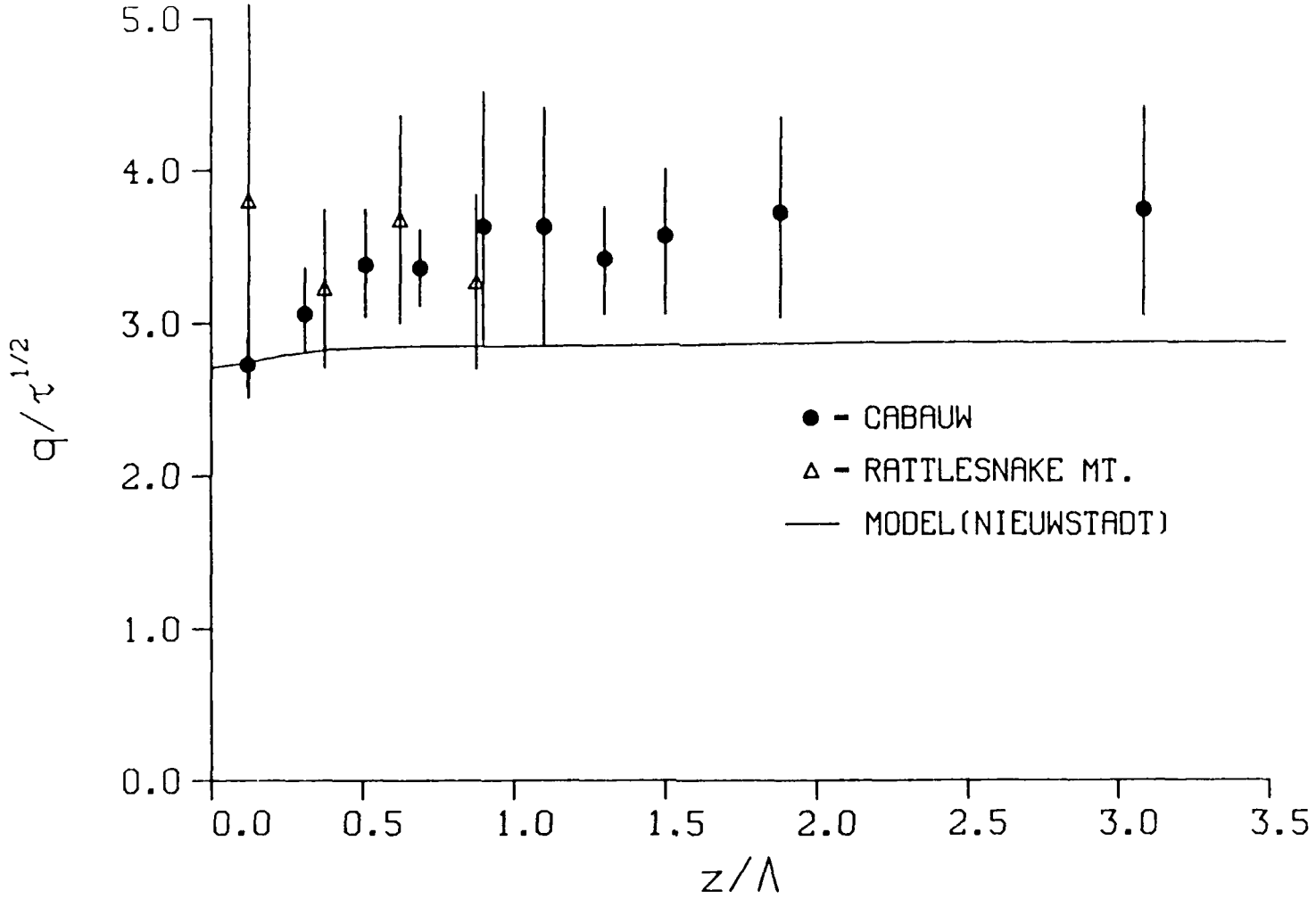

FIGURE 15. $q/\tau^{1/2}$ as a Function of z/Λ. Symbols Indicate Averages for Classes of z/Λ, and Vertical Bars Indicate Standard Deviations.

TABLE A-2. Spectral Transfer Functions for a Sonic Anemometer on a 21° Slope Oriented at 16.5° to the Downslope Direction. Downwind and crosswind components are in the plane parallel to the slope, and the vertical wind component is normal to the slope. θ is the mean wind direction relative to the downslope direction.

Downwind Component

k x	θ =-45°	θ =-30°	θ =-15°	θ = 0°	θ = 15°	θ = 30°	θ = 45°
0.16	0.975	0.979	0.982	0.980	0.975	0.973	0.976
0.32	0.930	0.942	0.950	0.945	0.933	0.927	0.935
0.64	0.828	0.862	0.884	0.873	0.846	0.830	0.844
1.28	0.702	0.790	0.839	0.811	0.751	0.699	0.693
2.56	0.538	0.624	0.644	0.611	0.559	0.500	0.463
5.12	0.194	0.187	0.181	0.203	0.214	0.205	0.201
10.24	0.101	0.078	0.044	0.090	0.102	0.092	0.095
20.48	0.033	0.027	0.021	0.030	0.034	0.030	0.035
40.96	0.015	0.014	0.010	0.014	0.016	0.015	0.016

Crosswind Component

k x	θ =-45°	θ =-30°	θ =-15°	θ = 0°	θ = 15°	θ = 30°	θ = 45°
0.16	0.996	0.994	0.994	0.995	0.996	0.999	1.003
0.32	0.986	0.983	0.983	0.984	0.984	0.989	1.000
0.64	0.947	0.950	0.955	0.953	0.945	0.948	0.967
1.28	0.829	0.861	0.884	0.870	0.832	0.819	0.850
2.56	0.597	0.680	0.725	0.687	0.606	0.569	0.619
5.12	0.307	0.436	0.495	0.409	0.273	0.230	0.312
10.24	0.104	0.206	0.262	0.189	0.084	0.054	0.114
20.48	0.036	0.083	0.110	0.077	0.031	0.020	0.044
40.96	0.017	0.035	0.045	0.033	0.014	0.010	0.019

Vertical Wind Component

k x	θ =-45°	θ =-30°	θ =-15°	θ = 0°	θ = 15°	θ = 30°	θ = 45°
0.16	1.000	1.002	1.002	1.001	1.001	0.998	0.993
0.32	1.000	1.003	1.001	0.999	1.000	0.996	0.985
0.64	0.990	0.987	0.976	0.972	0.978	0.980	0.966
1.28	0.883	0.841	0.808	0.808	0.838	0.873	0.866
2.56	0.590	0.542	0.525	0.525	0.546	0.597	0.652
5.12	0.361	0.350	0.338	0.342	0.342	0.352	0.382
10.24	0.151	0.145	0.145	0.143	0.146	0.155	0.176
20.48	0.037	0.027	0.025	0.034	0.044	0.053	0.066
40.96	0.023	0.021	0.017	0.018	0.022	0.025	0.029

configuration of the 1.9-m sonic anemometer on Rattlesnake Mountain that was used to estimate viscous dissipation. Here the mean wind direction θ is measured relative to the downslope direction: $\theta = 0°$ for a wind blowing straight down the slope and $\theta = -16.5°$ for a downslope wind along the sonic U axis.

TABLE A-1. Spectral Transfer Functions for Horizontal Flow. (θ is the mean wind direction relative to the sonic U axis.)

	Downwind Component			
$k\ell$	$\theta = 0°$	$\theta = 15°$	$\theta = 30°$	$\theta = 45°$
0.16	0.997	0.993	0.987	0.985
0.32	0.988	0.978	0.962	0.956
0.64	0.955	0.930	0.893	0.878
1.28	0.844	0.792	0.721	0.693
2.56	0.516	0.474	0.405	0.377
5.12	0.038	0.140	0.163	0.146
10.24	0.021	0.058	0.081	0.062
20.48	0.003	0.021	0.026	0.017
40.96	0.001	0.007	0.010	0.008

	Crosswind Component			
$k\ell$	$\theta = 0°$	$\theta = 15°$	$\theta = 30°$	$\theta = 45°$
0.16	0.994	0.995	0.995	0.995
0.32	0.984	0.984	0.984	0.983
0.64	0.955	0.953	0.948	0.945
1.28	0.882	0.872	0.846	0.831
2.56	0.731	0.692	0.608	0.563
5.12	0.499	0.415	0.263	0.192
10.24	0.269	0.197	0.083	0.039
20.48	0.117	0.083	0.031	0.013
40.96	0.048	0.036	0.014	0.006

	Vertical Wind Component			
$k\ell$	$\theta = 0°$	$\theta = 30°$	$\theta = 60°$	$\theta = 90°$
0.16	0.995	0.995	0.994	0.994
0.32	0.985	0.984	0.984	0.984
0.64	0.957	0.956	0.955	0.955
1.28	0.887	0.886	0.883	0.882
2.56	0.738	0.735	0.732	0.731
5.12	0.500	0.498	0.499	0.499
10.24	0.244	0.250	0.262	0.269
20.48	0.047	0.075	0.100	0.117
40.96	0.019	0.031	0.043	0.048

The principal assumption of this analysis is that the three-dimensional spectral density tensor can be described by the inertial subrange expression

$$\Phi_{ij}(k_1, k_2, k_3) = A\,\varepsilon^{2/3} k^{-5/3}(k^2\delta_{ij} - k_i k_j)/k^4 \qquad \text{(A-1)}$$

where k is the magnitude of the wave vector with components k_i, ε is the viscous dissipation rate, and A is a constant which need not be specified here. This assumption is entirely appropriate, since our main reason for correcting the spectra was to calculate the dissipation using the one-dimensional version of this expression. The inertial subrange spectral density was also used to correct the data for aliasing caused by digital sampling of the sonic data. A second assumption is that transfer functions calculated for one-dimensional wave number spectra can be applied to the measured frequency spectra through the use of Taylor's hypothesis

$$k_1 = 2\pi n/u\ , \qquad \text{(A-2)}$$

where k_1 is the wave number in the direction of the mean wind u_1, and n is frequency. This assumption is usually valid in the atmosphere for the high wave number, inertial subrange of the spectrum; this assumption was also necessary to calculate dissipation rates from the measured spectral densities.

Tables A-1 and A-2 list the calculated power spectral transfer functions for the three wind components, as a function of wave number k normalized by the path length ℓ. Table A-1 lists the transfer functions for horizontal flow (flow normal to the vertical sonic axis) as a function of the mean wind direction θ measured relative to the sonic U axis. The horizontal transfer functions are symmetrical at 45° intervals, and the vertical transfer function is symmetrical at 90° intervals. The one-dimensional spectral density tensor is obtained by integrating the three-dimensional spectral densities over the components of the wave number vector normal to the mean wind direction, k_2 and k_3. As a consequence, the transfer functions for the downwind component are noticeably different from those for the crosswind and vertical components.

Table A-2 lists the transfer functions for an anemometer on a 21° slope, oriented at 16.5° relative to the downslope direction. This was the

APPENDIX

CORRECTION OF SONIC ANEMOMETER DATA FOR SPATIAL AVERAGING

A sonic anemometer measures the speed of the wind by transmitting sound waves between a pair of acoustic transducers. The wind component along a sonic path, defined by the line connecting a transducer pair, is determined from the difference in transit times for sound waves transmitted in opposite directions along that path. In order to measure all three components of the wind vector, the sonic anemometers used in this study have three orthogonal paths, each of which is 25 cm long and is actually composed of two parallel paths (to allow simultaneous measurement of the transit time in both directions) separated by 2.5 cm. The two horizontal axes cross at their centers, but are separated vertically by 4.45 cm. The vertical axis is in the same vertical plane as the horizontal U axis, and its center is separated by 33.18 cm horizontally and 28.65 cm vertically from the midpoint of the two horizontal axes.

In order to use a sonic anemometer to measure eddies with wavelengths comparable to the anemometer's dimensions, we must consider the effects of path averaging and path separation on its response. Kaimal et al. [1] present a detailed derivation of the required spectral transfer functions, the ratio of the measured to the actual one-dimensional power spectra, for the three components of the wind as measured by a sonic anemometer. Horst [2] extended their calculations to account for additional spatial separations, which were originally neglected.

The procedures of Kaimal et al. [1] and Horst [2] were further extended to calculate spectral transfer functions for the sonic anemometers used in this study. This was necessary because the geometry of our anemometers is different from that used for the Kaimal et al. and Horst calculations and because those calculations assumed that the flow was normal to the vertical axis of the anemometer. Our anemometers were aligned with the true vertical but the flow was roughly parallel to the slope, increasing the complexity of the transfer function calculation.

LITERATURE CITED

1. J. C. Doran and T. W. Horst. 1981. "Velocity and Temperature Oscillations in Drainage Winds." J. Appl. Meteor. 20:361-364.

2. A. J. Garrett. 1983. "A Drainage Flow Prediction With a One-Dimensional Model Including Canopy, Soil and Radiation Parameterization." J. Appl. Meteor. 22:79-91.

3. K. S. Rao and H. F. Snodgrass. 1981. "A Nonstationary Nocturnal Drainage Flow Model." Bound.-Layer Meteor. 20:309-320.

4. J. C. Doran and T. W. Horst. 1983. "Observations and Models of Simple Nocturnal Slope Flows." J. Atmos. Sci. 40:708-717.

5. T. Yamada. 1983. "Simulations of Nocturnal Drainage Flows by a $q^2 \ell$ Turbulence Closure Model." J. Atmos. Sci. 40:708-717.

6. P. C. Manins and B. L. Sawford. 1979. "A Model of Katabatic Winds." J. Atmos. Sci. 36:619-630.

7. D. R. Fitzjarrald. 1984. "Katabatic Wind in Opposing Flow". J. Atmos. Sci. 41:1143-1158.

8. P. C. Manins and B. L. Sawford. 1979. "Katabatic Winds: A Field Case Study." Quart. J. Roy. Meteor. Soc. 105:1011-1025.

9. F. T. M. Nieuwstadt. 1984. "The Turbulent Structure of the Stable, Nocturnal Boundary Layer." J. Atmos Sci. 41:2202-2216.

10. R. T. McNider and R. A. Pielke. 1984. "Numerical Simulation of Slope and Mountain Flows." J. Appl. Meteor. 23:1441-1453.

11. J. C. Wyngaard and O. R. Cote. 1971. "The Budgets of Turbulent Kinetic Energy and Temperature Variance in the Atmospheric Surface Layer." J. Atmos. Sci. 28:190-201.

12. J. C. Kaimal, J. C. Wyngaard, Y. Izumi and O. R. Cote. 1972. "Spectral Characteristics of Surface-Layer Turbulence." Quart. J. Roy. Meteor. Soc. 98:563-589.

13. J. C. Kaimal, J. C. Wyngaard and D. A. Haugen. 1968. " Deriving Power Spectra from a Three-Component Sonic Anemometer." J. Appl. Meteor. 7:827-837.

14. T. W. Horst. 1973. "Spectral Transfer Functions for a Three-Component Sonic Anemometer." J. Appl. Meteor. 12:1072-1075.

15. J. C. Wyngaard, O. R. Cote and Y. Izumi. 1971. "Local Free Convection, Similarity and the Budgets of Shear Stress and Heat Flux." J. Atmos. Sci. 28:1171-1182.

PUBLICATIONS AND PERSONNEL

"Turbulence Structure of Nocturnal Slope Winds," by J. C. Doran and T. W. Horst was presented at the Fourth Joint Conference of Air Pollution Meteorology and Third Conference on Mountain Meteorology, October 16-19, 1984, in Portland, Oregon, and appeared in the conference preprints.

"Nocturnal Drainage Winds on Simple Slopes," by T. W. Horst and J. C. Doran has been accepted for publication by Boundary-Layer Meteorology. Most of the work discussed in this paper was funded by the U.S. Department of Energy, but some of the findings of the 1983 experiments, funded by the Army Research Office, have been included.

"A Turbulent Kinetic Energy Budget in Nocturnal Slope Flow," by T. W. Horst and J. C. Doran will be submitted for presentation at the Seventh Symposium on Turbulence and Diffusion in November 1985.

"Turbulence Characteristics of Drainage Winds Over a Simple Slope," by J. C. Doran and T. W. Horst is being prepared and will be submitted for publication to Boundary-Layer Meteorology.

During the course of this work, J. C. Doran and T. W. Horst were the principal scientific personnel supported by project funds. Technical support was provided by O. B. Abbey, G. W. Dennis, and J. W. Buck.

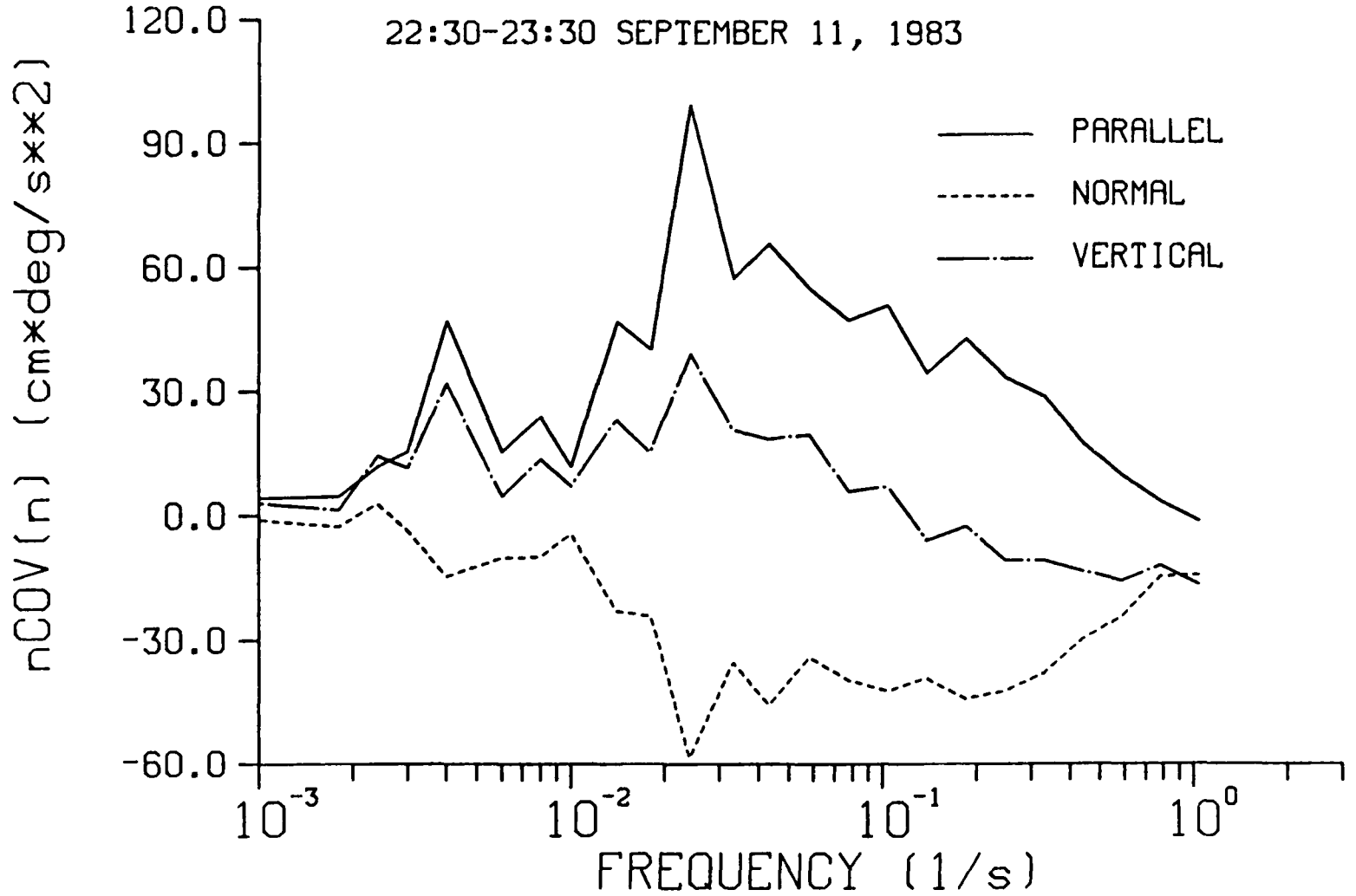

FIGURE 17. Cospectra of w and T at 1.9 m. "Parallel" Values Have Been Multiplied by -sinβ, and "Normal" Values Have Been Multiplied by cosβ, where β is the Slope Angle.

analyzed the energy budget, the parallel heat flux above the jet was three times the normal heat flux. For our 21° slope, therefore, the contributions of the two heat flux components to the buoyancy term in the energy budget almost cancel each other. In other words, the vertical heat flux is small (and in most cases actually positive) because the vertical components of the parallel and normal heat fluxes are comparable. This cancellation is illustrated in Figure 17, which shows cospectra of the net vertical heat flux and of the vertical components of the parallel and normal heat fluxes. The normal and parallel components of the buoyancy term are generally on the order of 6 cm^2/s^3, about 15% of the shear production term, but the net buoyancy term averages 1.1 cm^2/s^3, only 3% of the shear production term.

The imbalance in the turbulent kinetic energy budget ranges from -7 to 22 cm^2/s^3, with an average imbalance of 7.3 ± 11.5 cm^2/s^3. The imbalance is 19% of the shear production term, but it is comparable to the statistical uncertainty in the shear production and viscous dissipation terms. The net buoyancy term makes a statistically negligible contribution to the energy budget. Neither is there any evidence that divergence of the vertical flux of turbulent kinetic energy or pressure transport make a significant contribution to the energy budget, unless the large (43 to 48%) imbalance for some individual 10-min periods is related to intermittent turbulent energy flux divergence or pressure transport. Thus the energy budget above the jet is essentially a balance between shear production and viscous dissipation. Below the jet, both the normal and along-slope buoyancy terms are energy sinks, and therefore we would expect the net buoyancy term to be noticeably more important in that region, perhaps contributing as much as 30% of the energy budget.

the dissipation rate were constant with frequency within 10 to 30%. The 10-min estimates of the dissipation rate varied from 25 to 40 cm^2/s^3, with an average for the hour of 32.2 ± 6.4 cm^2/s^3.

The buoyancy term in the energy budget is $(g/T)\overline{u_3\theta}$, where u_3 is the true vertical wind component. We find that this term is quite different in slope flow from that over flat terrain and that it can be either a source or a sink for turbulent kinetic energy, depending on the slope angle and whether one is below or above the wind speed maximum. The buoyancy term can be divided into components normal and parallel to the slope,

$$(g/T)\overline{u_3\theta} = (g/T)\overline{w\theta}\cos\beta - (g/T)\overline{u\theta}\sin\beta \qquad (7)$$

where β is the slope angle, w is the fluctuating velocity component normal to the slope, and u is the component parallel to the slope. The heat flux $\overline{w\theta}$ normal to the slope is negatives and thus the first term on the right-hand side of Equation (7) is always a sink for turbulent energy. The heat flux $\overline{u\theta}$ parallel to the slope is a consequence of the momentum and heat fluxes normal to the slope; i.e., because $\overline{uw}$ and $\overline{w\theta}$ are nonzero, $\overline{u\theta}$ is expected to be nonzero as well. Under stable conditions over flat terrain, the vertical momentum and heat fluxes are both negative, and the horizontal heat flux is positive (but makes no contribution to the energy budget). Similarly, in the region below the wind speed maximum where the fluxes of momentum and heat normal to the slope are both negative, the heat flux parallel to the slope is positive (downslope). Above the jet, however, the momentum flux is positive and the heat flux parallel to the slope is negative (upslope). Thus the last term in Equation (7) is a sink for turbulent kinetic energy below the jet and a source above.

The net contribution of the normal and parallel heat flux components to the kinetic energy budget depends on the slope angle and the relative magnitudes and signs of the heat flux components. Under stable conditions over flat terrain, the horizontal heat flux is 2 to 10 times larger than the vertical heat flux [9, 15]. Similarly, we find that the parallel heat flux component is several times the normal heat flux. During the period for which we

TABLE 3. Turbulent Kinetic Energy Budget for Sept. 11, 1983, 22:30 to 23:30. T: 10-min subperiods; P: shear production; D: viscous dissipation; B: buoyant production; I: budget imbalance. Units are cm^2/s^3.

T	P	D	B	I
1	34.2	40.6	-0.5	-6.9
2	41.7	38.8	1.3	4.2
3	40.9	24.8	3.5	19.6
4	33.8	27.1	0.5	7.2
5	50.2	29.3	0.8	21.7
6	29.3	32.4	1.0	-2.1
Average	38.4	32.2	1.1	7.3

The generalized shear production term is $\overline{u_i u_j}\, dU_i/dx_j$. In a coordinate system with its axes aligned normal and parallel to the slope this term is $\overline{uw}\, dU/dn + \overline{vw}\, dV/dn$. For each 10-min period, the wind shear was determined from propeller anemometers above and below the 1.9-m sonic, and the momentum fluxes were determined from the covariance of the deviations of the individual velocity components from the 10-min average. The 10-min estimates varied from 30 to 50 cm^2/s^3, with an average for the hour of 38.4 ± 7.5 cm^2/s^3. In most cases, this is the dominant term in the energy budget.

The dissipation was determined from the velocity spectra of the streamwise wind component in the inertial subrange, using the Kolmogorov law

$$n\phi_u(n) = \alpha_1 \varepsilon^{1/2} (2\pi n/u)^{-2/3} \qquad (6)$$

where n is frequency, $\phi_u(n)$ is the one-dimensional spectrum of the mean velocity fluctuations, α_1 is the one-dimensional Kolomogorov constant equal to 0.50 [12], and ε is the dissipation rate. Because the inertial subrange occurs at the high frequency end of our measured spectra, it was necessary to correct the sonic data for spatial averaging and aliasing as discussed by Kaimal et al. [13] and Horst [14]. Transfer functions calculated specifically for the sonic anemometers used in this study are tabulated in the Appendix. After correction of the sonic spectra, the predicted -2/3 dependence of the spectral density on frequency was found to hold above 0.2 Hz, and estimates of

TURBULENT KINETIC ENERGY BUDGET

The preceding discussion of the turbulence structure of slope flow implied that the turbulent kinetic energy was proportional to the local vertical wind shear. This assumption was based on the known properties of the turbulent kinetic energy budget for stably stratified flow over flat terrain. We have been able to measure directly the dominant terms in the turbulent kinetic energy budget in slope flow and establish that the energy budget is similar to that over flat terrain.

Under stable conditions over flat terrain the dominant terms in the turbulent kinetic energy budget are shear production and viscous dissipation [11]. Under stable conditions buoyant production is a sink for turbulent energy, but it is never more than 20% of the shear production term. Divergence of the vertical turbulent flux of kinetic energy has been found to make an even smaller contribution to the energy budget. Thus the stable kinetic energy budget is essentially a balance between shear production and dissipation, with an additional small loss of energy caused by buoyancy. Wyngaard and Cote [11] found that observations of these three terms for stable conditions over flat terrain produced a turbulent kinetic energy budget that balanced within about 30 to 35% of the dissipation rate. They felt that the remaining imbalance could be attributed to experimental uncertainties in measuring the individual terms.

The turbulent kinetic energy budget for slope flow was estimated from the data for September 11, 1983, 22:30 to 23:30. Meteorological conditions were quite stationary during this time period. The maximum wind speed was measured at a height of 1 m, and thus the 1.9-m sonic anemometer data could be used to determine the energy budget for the region of negative shear above the jet that is a distinctive characteristic of slope flow. The shear production and buoyancy terms in the budget were determined from direct measurements of the momentum flux, the wind shear, and the heat flux, and the dissipation was estimated from the inertial subrange of the velocity spectrum of the mean wind component parallel to the slope. Table 3 shows these terms for six consecutive 10-min periods and for the 1-h average.

We conclude that local scaling seems to be a promising approach to the description of turbulence in drainage flows, although a more rigorous test of this approach requires additional measurements over a wider range of z/Λ values; more theoretical justification would also be welcome. It seems plausible that the decoupling of the flows above the jet from the surface means that the surface similarity theory often applied over flat terrain is inapplicable to slope flows. Below the jet, surface similarity theory might still be useful, but, in the region of the jet, quantities that depend on wind speed gradients are likely to be ill-defined.

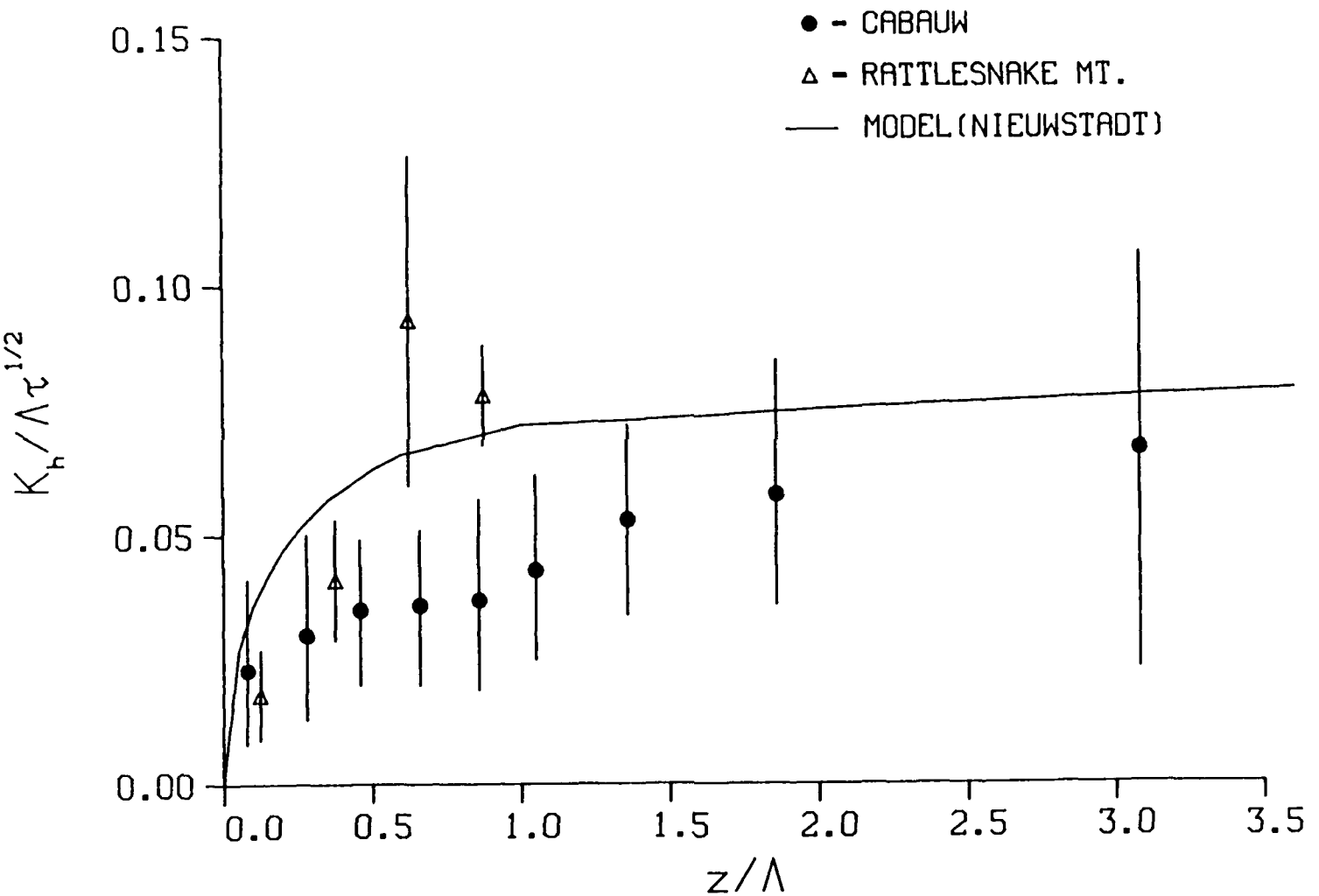

FIGURE 16. $K_h/\Lambda\tau^{1/2}$ as a Function of z/Λ. Symbols Indicate Averages for Classes of z/Λ, and Vertical Bars Indicate Standard Deviations.

and

$$K_m = \tau \Big/ \left\{ \left(\frac{\partial U}{\partial z}\right)^2 + \left(\frac{\partial V}{\partial z}\right)^2 \right\}^{1/2} \qquad (5)$$

In Figure 16 we show the variation of $K_h/\Lambda\tau^{1/2}$ with z/Λ, and compare these values with those of Nieuwstadt. Again, there is significant scatter. For our lowest two classes of z/Λ, there is good agreement between the Rattlesnake Mountain and the Cabauw data. For larger values of z/Λ, our results lie appreciably above the Cabauw measurements. Whether this trend continues for larger values of z/Λ is not known. Unfortunately, we are not able to extend our comparisons to larger values of z/Λ because of our limited range of measurements.

We noted earlier that determining velocity gradients in the region of the jet is difficult; because of this, dependable estimates are harder to obtain for K_m than for K_h. However, on the night of September 11-12, during a period of ~2 h the maximum observed wind speed was at our lowest anemometer (~1 m), and we were able to calculate somewhat more reliable estimates of the derivatives of the wind speed. For this time period, we found that the ratio K_m/K_h was 1.2 ± 0.35. Nieuwstadt's model and observations suggest that $K_h \cong K_m$, and our results are consistent with this result, within the experimental uncertainty.

Nieuwstadt's model, as well as his data, shows the Richardson number increasing with z/Λ for z/Λ less than 1 and then changing very little with z/Λ above z/Λ equal to 2. Our scatter was too large to allow a reasonable comparison of our Richardson number data with Nieuwstadt's findings, and we note that we had no value of z/Λ larger than about 1. Thus, we are unable to determine whether a constant value of Richardson number is approached in drainage flows. In contrast to the Richardson number behavior, Nieuwstadt's model and data show that quantities such as $q/\tau^{1/2}$ and $\tau_w/\tau^{1/2}$ should be independent of z/Λ at much lower values of z/Λ than are required for constancy of Ri. For these quantities, the evidence for the utility of local scaling of turbulence in slope flows is encouraging if not definitive.

LITERATURE CITED

1. J. C. Kaimal, J. C. Wyngaard and D. A. Haugen. 1968. " Deriving Power Spectra from a Three-Component Sonic Anemometer." J. Appl. Meteor. 7:827-837.

2. T. W. Horst. 1973. "Spectral Transfer Functions for a Three-Component Sonic Anemometer." J. Appl. Meteor. 12:1072-1075.

END

FILMED

8-85

DTIC